A Study of Double Glass Covered Trapezoidal Salt Gradient Solar Pond Coupled with Reflector

A Dissertation submitted
in partial fulfillment of the requirements for
the degree of

Master of Engineering

in

Thermal Engineering

by:

Sandeep Kumar

Registration No.: 801483022

Under the Supervision of

Dr. Madhup Kumar Mittal

MECHANICAL ENGINEERING DEPARTMENT

THAPAR UNIVERSITY, PATIALA

June, 2016

Certificate

I hereby declare that the thesis entitled "**A study of double glass covered trapezoidal salt gradient solar pond coupled with reflector**" is an authentic record of my work carried out as requirements for the award of the degree of **Master of Engineering** in **Thermal Engineering** at **Thapar University, Patiala** under the supervision of **Dr. Madhup Kumar Mittal**, Assistant professor, MED, Thapar University, Patiala during July, 2014 to July, 2016. No part of the matter embodied in this report has been submitted to any other university or institute for the award of any degree.

Date: 08/07/2016

Sandeep Kumar

It is certified that the above statement made by the student is correct to the best of my/our knowledge and belief.

Dr Madhup Kumar Mittal
MED
Thapar University, Patiala - 147004

Countersigned
by

Head, Mechanical Engineering Department
Thapar University, Patiala – 147004

Dean of Academic Affairs
Thapar University, Patiala - 147004

Dedication

I dedicate this thesis to my beloved father Rakesh Kumar and my mother Usha Rani, who are an ever supporting and encouraging with their great patience. I also dedicate this to my brother Lucky Bansal, who is as an impression for me and to all my dearest friends.

Acknowledgement

I would like to express my deep sense of gratitude to **Dr. Madhup Kumar Mittal,** Assistant Professor, Mechanical Engineering Department, Thapar University, Patiala for their invaluable suggestions, excellent supervision, constant encouragement and critical discussion throughout the work.

I am also thankful to **Dr. S. K. Mohapatra** , Professor and Head, Mechanical Engineering Department, Thapar University for providing me an opportunity to do my seminar work on the topic of my interest.

The greatest thanks go to my family for their infinite support. Besides, I would like to acknowledge my institute i.e. Thapar University.

Sandeep Kumar

SANDEEP KUMAR

Abstract

In this study, a trapezoidal salt gradient solar pond (TSGSP) having a top surface area of $1.625 \times 1.625\,m^2$ and bottom surface area of $0.71 \times 0.71\,m^2$ and depth of 0.90 m has been constructed to investigate the temperature distribution and thermal performance of TSGSP. The top surface of solar pond is covered with double glass cover in order to reduce the evaporative and convective losses from the top. A reflector made of aluminium sheet is used for enhancing the solar intensity on the top surface of the solar pond during sunny hours. The position of reflector is changed manually in steps to track the sun in order to receive maximum beam radiation on the reflector surface. This reflector is also used as a cover on the top surface of the solar pond to reduce the thermal losses during the night. The sunny area ratio of trapezoidal solar pond is calculated theoretically and compared with that of square solar pond. For the purpose of comparison of sunny area ratio between trapezoidal and square solar ponds, three cases of square solar ponds are considered in this study. These three cases of square solar ponds are: square solar ponds with the same surface area and volume, with the same surface area and height and with the same height and volume as that of trapezoidal solar pond. The experimental results show that the average temperature of solar pond without double glass cover is 44.2 °C and this temperature increased to 55°C when solar pond is covered with double glass cover. The use of reflector with fixed position and with changing position enhances the average solar intensity on the top surface of solar pond by 22% and 47%, respectively. The thermal efficiencies of LCZ, NCZ and UCZ for the trapezoidal solar pond with double glass cover and reflector are estimated to be 32.73%, 23.22% and 5.30%, respectively. The results of theoretical analysis provide an information that the trapezoidal solar pond and the square solar ponds with the same surface area and volume, with the same surface area and height and with the same height and volume as that of trapezoidal solar pond have highest sunny area ratio of 94.12%, 88.86%, 84.2% and 78.6% respectively in the month of June, 2016.

Key words: Trapezoidal solar pond; Glass cover; Reflector cover; Shading areas; Temperature distribution.

Contents

List of figures

List of Tables

Nomenclature

S_I	decrease the length of a solar pond due to the trapezoidal shape of the solar pond
Sh_I	shading length of the Ith layer in the solar pond, m
Δx	thickness of each layer, m
x	depth of water, m
E	Total solar energy on the top surface of solar per unit area, W/m^2
L_W	width of the square solar pond, m
L_{WI}	width of Ith layer for TSGSP, m
A_{sh}	the shading area of the solar pond, m^2
A_{sur}	surface area of solar pond, m^2
A_{su}	Sunny area of solar pond, m^2
n	day of the year
l	Length of the reflector
V	volume of solar pond for particular zone, m^3
C_P	specific heat capacity, J/kg°C
Q_{Solar}	the net solar energy reached to the surface of solar pond, W/m^2
h	local solar time
ΔZ_{UCZ}	thickness of UCZ
ΔZ_{LCZ}	thickness of LCZ
C	Concentration of water, Kg/m^3
s	Salinity, g/kg
T	temperature of saline water, °C
T_i	initial temperature of saline water, °C
T_f	final temperature of saline water, °C
T_{NCZ}	temperature of NCZ, °C
T_{UCZ}	temperature of UCZ, °C

Greek letters

α	elevation angle
β	fraction of radiation that enters in the solar pond
γ_1	angle between the line joining the top end of reflector and extreme end point of pond
γ_2	angle between the reflected solar rays and horizontal surface of the solar pond
δ	thickness at which long wavelength is absorbed
i	incidence angle of solar radiation with the normal reflector surface
θ	inclination angle of reflector
θ_i	incidence angle of solar radiation with the normal solar pond surface
θ_{rf1}	refraction angle when solar radiation pass through air to glass
θ_{rf2}	refraction angle when solar radiation pass through air to water
θ_z	zenith angle
θ_h	hour angle
φ	latitude angle
δ_d	declination angle
ρ	density of saline water, Kg/m^3
τ	transmittance

Acronyms

TSGSP	trapezoidal salt gradient solar pond
TSP	trapezoidal solar pond
UCZ	upper convective zone
NCZ	non-convective zone
LCZ	lower convective zone
SSP	square solar pond

Chapter 1

Introduction

1.1 Introduction

Solar radiations consists a large amount of energy source, solar energy is available in all parts of the earth. The solar pond is the best way to collect and store the solar energy coming from solar radiation. This solar energy should be used for different applications such as water desalination, drying, refrigeration, space heating & power generation [2]. Von Kalecsinsky in the early 1900, the phenomenon of solar pond was discovered in Medve Lake in Transylvania [3]. Solar pond absorbs the heat from solar energy due to wavelength dependent absorption and transmission coefficient of water. Solar radiations coming from the sun are of short wavelength for which absorption/emission coefficient of water is low & its transmission coefficient is high. The solar radiations reach to the bottom of a pond and increase its temperature. The bottom surface of pond in turn radiate radiations of long wavelength for which absorption/emission coefficient of water is high and its transmission coefficient is low. In ordinary lakes, the water is heated by solar energy and heated water rise to the surface of a lake and then losses the heat to the environment. But, in salt gradient solar pond, the convection currents are smothered by increasing the density of water at the bottom.

Generally, the solar ponds are comprises of three distinct zones which are as follows; the first zone, known as upper convective zone (UCZ), is the fresh water layer situated at the top of the pond. In this zone, the density of water is almost equals to the density of fresh water. The second zone, known as the non-convective zone (NCZ), is an important zone because this zone suppresses the convection currents in the solar pond and thus prevents the heat losses from the surface of pond. This zone consists of salty water layers having the concentration of salt gradually increasing towards the bottom side. The solar radiations from the sun penetrate through this zone. The third zone, the lower convective zone (LCZ) is also known as heat storage zone. The density, temperature and concentration of saline water is maximum in this zone and remain constant throughout the zone.

The thermal energy balance and thermal stability of salt gradient solar pond was first investigated by Weinberger [4]. In salt gradient solar pond, different types of salt are used

such as sodium chloride (NaCl), sodium carbonate (Na_2CO_3), magnesium chloride ($MgCl_2$) etc. Kurt et al.[5] analysed the experimentally and numerically of salt gradient solar pond by using sodium carbonate of. Bozkurt et al.[6] carried out performance estimate of magnesium chloride salt gradient solar pond. Mazidi et al. [7] studied the wall shading effects on the performance of solar pond by the two-dimensional modelling. Al-Dabbas [8] formulate the mathematical model to bode the performance of salt gradient solar pond in different seasons. The experimental and theoretical study of temperature distribution was done by Karakilcik et al. [9]. Sakhrieh and Al-Salaymeh [10] have developed the MATLAB code for the prediction of a temperature distribution of solar pond. Karakilcik et al. [11] performed the experimental evaluation of energy allocation and energy efficiencies for the solar pond with shading effect and without shading effect. Karakilcik et al. [12], [13] evaluated the effect of sunny area ratio on the efficiency of solar pond. Bezir et al. [14], [15] experimentally and theoretically analysed the performance of solar pond with and without reflector. They concluded that the performance of solar pond with reflector is increased by 25% as compared to that of solar pond without reflector. The evaporation losses are the major losses from the top surface of a solar pond and these losses can be decreased by using cover at the top surface. Bozkurt et al. [16] used three different types of transparent cover surfaces on the top surface of solar pond and found that the highest efficiency of a solar pond was 17.86% with glass cover. Ramadan and Khallaf [17] used double glass cover with mini shallow solar pond to reduce top losses due to convection. Husain et al. [18] determined culminated thickness of non-convective zone for solar pond. Saxena et al. [19]studied the effect of water depth on the performance of solar pond.. Dehghan et al. [20] perform an experimental investigation with square and circular solar ponds and observed that circular solar pond was more efficient than the square solar pond.

In this study, a trapezoidal salt gradient solar pond has been constructed and its thermal performance has been investigated for three configurations, i.e., without double glass cover and without reflector, with double glass cover and without reflector and with double glass cover and with reflector. The reflector is kept at an angle at which the reflector reflects the maximum solar radiation on the surface of the solar pond. In order to receive the maximum solar radiation on the reflector surface throughout the day, the reflector is positioned east facing during 9 am to 11 am, south facing during 11 am to 2 pm and west facing during 2 pm to 5 pm. The temperature distribution of UCZ, NCZ and LCZ has been measured for the above mentioned three configurations of TSGSP. Further, the shading areas

in UCZ, NCZ and LCZ of TSGSP with double glass cover have been theoretically determined. The shading areas in distinct zones of different square solar ponds having the same surface area and volume, same height and surface area and same height and volume as that of TSGSP are also determined and compared with the shading areas in corresponding zones of TSGSP.

1.2 Types of Solar Pond

Solar pond can be classified as given below in figure 1.1

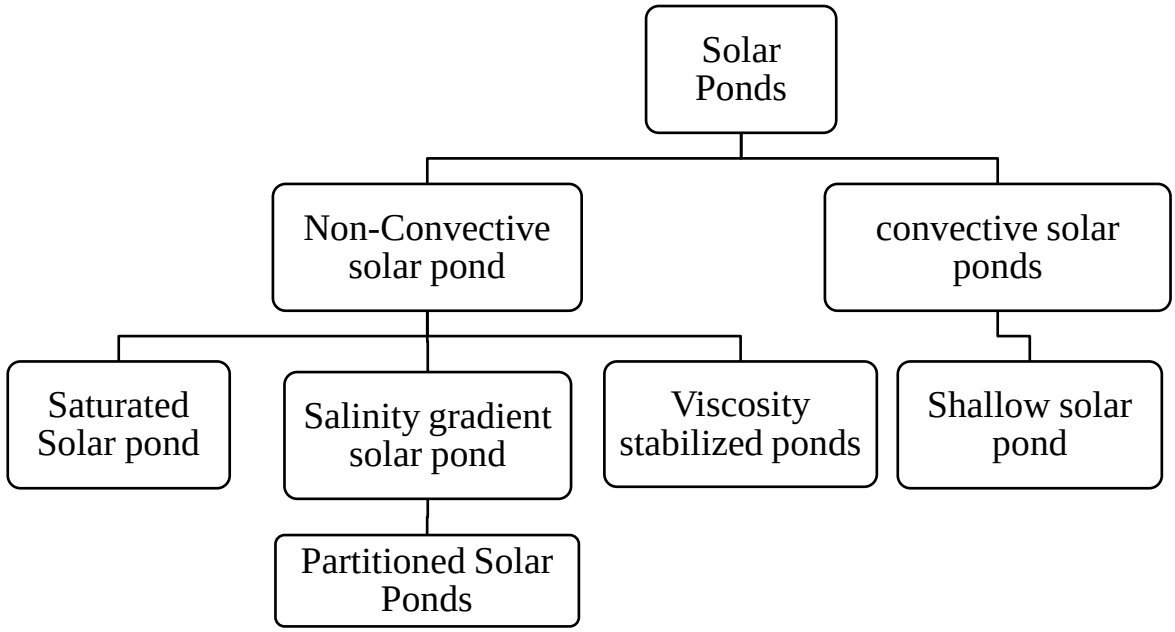

Figure 1.1 Classification of Solar Ponds [1]

1.2.1 Convective solar pond

The convection solar pond is also termed as shallow solar pond. It consists of a large bag that prevents evaporation but permits convection. The bag has blackened bottom with foam insulation below, and two types of glazing (sheets of plastic or glass) on top. Solar energy heats the water in the bag during the day and at night the hot water is pumped into a large heat storage tank to minimize heat loss. Another type is the deep, salt less pond. Double glazing covers deep salt less pond. When solar energy is not available or at night placing insulation on the top of the glazing reduces heat loss.

1.2.2 Non-Convective solar pond

A non-convective solar pond is a large shallow body of water 1 to 5 m deep, but 3-4 m on the average, which is arranged in a way so that the temperature gradient is reversed from the normal. This allows collection of radiant energy into heat (up to 95 °C), storage of heat and transport of thermal energy, at temperature 40-50 °C above normal, out of the system. There are three types of non-convective solar ponds in terms of the methods of maintaining layered structure. One is SGSP where density gradient is maintained by salt water. The other is membrane solar pond which uses horizontal and vertical membranes. The third one is polymer gel layers solar pond. A non-convective solar pond is depicted in figure 1.2

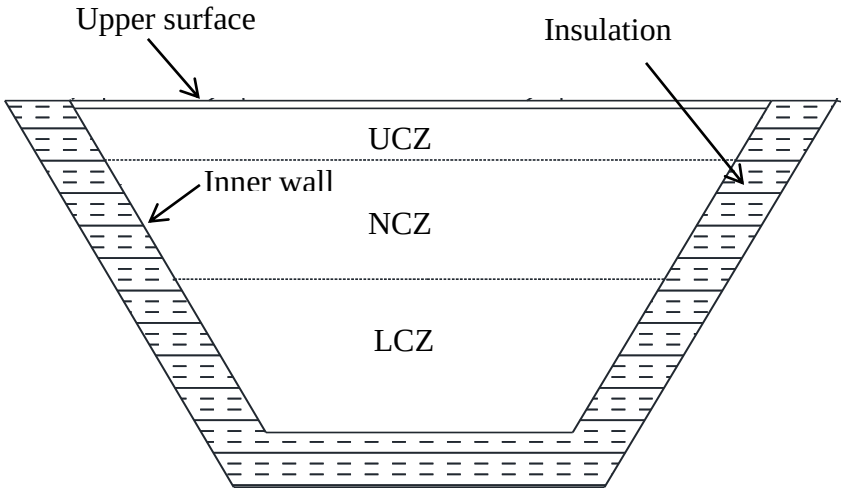

Figure 1.2 Non-Convective solar pond

1.2.2.1 Saturated Solar Ponds

Saturated Solar ponds are filled with salt up to the depth of the pond. The concentration of salt changes because the density inside the solar pond changes. Solubility of salt in water will increase due to the increase in the temperature of saline water. Water cannot rise to Solar Ponds of the surface because water is heating in the bottom of the pond and increases its solubility and therefore it will not lose its heat content. The choice of salt in such a way density would increase with temperature otherwise some kinds of salt make the solution decrease its density from a certain temperature on which would destroy the pond's performance.

1.2.2.2 Salt gradient solar pond

A salt gradient solar pond has three distinct layers of brine of varying concentrations. The key point of the salt gradient solar pond is salinity in water of solar pond was continuous increasing towards the bottom. The salinity and density of different layers of the pond is increases with the depth that's why this solar pond is known as salinity-gradient solar ponds.

- The first zone is Upper Convective Zone (**UCZ**), UCZ is filled with fresh to maintain the density of water as close to density of fresh water. The upper convective zone lies on the top of solar pond therefore temperature of this zone is nearly closed to ambient temperature and energy loss takes place from convection and evaporations. Top layer requires continuous flushing of fresh water to take care of evaporation.
- The second zone is Non-Convective Zone (**NCZ**), is just below the upper convective layer. Salt concentration is increasing with depth and salt concentration was measured from the interface of UCZ and NCZ. The NCZ is the key zone in the working of a solar pond. It allows a large solar radiation to penetrate through the NCZ to the storage zone.
- The last and third zone is Lower Convective Zone (LCZ) also called as Heat Storage Zone (HSZ) of the solar pond. LCZ is made up of salinity water layers with the highest temperature and highest density. Some amount of the solar radiation reaches the storage zone of the pond and particular layer of saline water is heated then slightly reduced the density of this layer but remains the density of this layer is higher than its above layer, therefore convection current is suppressed in the LCZ.

1.2.2.3 Partitioned Solar Ponds

Partitioned solar pond has three distinct layers and these layers are separated with transparent membranes LCZ is separated from NCZ to diminish its effect on the NCZ for increase the temperature inside HSZ therefore performance of the solar pond will increase. The membrane is used are transparent otherwise less amount of solar radiation reach to bottom surface of the solar pond. If the stress takes place in the membrane due to thermal expansion of the HSZ or the gravitational pressure of the NCZ then there will be possibility of fracture in the membrane. If the HSZ cools down or if heat is taken out of the HSZ a negative thermal expansion will occur. If fracture in the membrane occurs then the performance of the pond will decrease and cause mixing of the layers.

1.2.2.4 Viscosity Stabilized Solar Ponds

A particular gel is used to thick the water which reduces the convection losses. The amount of gel is very high, as to enough increasing thickness of water to avoid convection but also keeps its temperature resistance. The gel should be used are transmittance otherwise it will reduce the thermal performance of solar pond. Additionally, it should have a good physical resistance to control precipitation.

1.3 Solar radiation geometry

Zenith angle (θ) is the angle between the normal to the surface and an incident radiation of beam. The angle θ is related with the general equation in which β is the slope, φ latitude angle, δ the declination angle, γ_H the surface azimuth angle and ω the hour angle.

Latitude Angle (φ): The angle made by the line joining the location of the centre of the earth with the projection of the line on the equatorial plane. The latitude was measured negative for the southern hemisphere and as positive for the northern hemisphere; $-90° \leq \varphi \leq 90°$.

Slope (β): The angle made by the plane surface with the horizontal surface; $0° \leq \beta \leq 180°$.

Surface Azimuth Angle (γ_H): Angle made in the horizontal plane between horizontal line due south and the projection of normal to the surface on the horizontal plane; $-180° \leq \gamma_H \leq 180$.

Declination (δ_d): The angle made by the line joining the centres of the Earth and the Sun with the projection of this line joining on the equatorial plane; $-23.45° \leq \delta_d \leq 23.45°$.

Hour Angle (θ_h): The angular measurement of time and is equals to 15° per hour$-90° \leq \theta_h \leq 90°$.

1.4 Research Objectives

An experimental work has been carried out to investigate the performance of trapezoidal salt gradient solar pond under varying conditions of solar radiation and ambient temperature with the following objectives

1. To fabricate a trapezoidal salt gradient solar pond.
2. To determine the temperature distribution in various zones of trapezoidal salt gradient solar pond.
3. To determine the thermal performance of trapezoidal salt gradient solar pond.

4. To compare the thermal performance between trapezoidal salt gradient solar pond without reflector and trapezoidal salt gradient solar pond coupled with reflector.
5. To theoretically determine the shading area in different zones of trapezoidal salt gradient solar pond.

Chapter 2

Literature review

Gomes J. et al. [2] represents the small amount of power generation with the help of thermoelectric generators in which heat was taken from the salinity-gradient solar pond. In this system, the heat energy was converted into electrical energy with the help of 16 TEG's (thermoelectric generators), which works on the principle of see-back effect. See-back effect works when the temperature difference maintains and this temperature difference was created with the help of cold and hot water of salinity gradient solar pond. As the temperature difference creates then voltage will generate because voltage generated between two junctions was directly proportional to the temperature difference of the heat sink and heat source. If higher the voltage would create than the temperature difference must be high. Results showed that the maximum power is generated when the temperature difference created 100 ºC across the 16 thermoelectric generators and power generated was 9.56 W at voltage of 15.67 V and at current is 0.6. They concluded maximum power was obtained when the resistance of of all the 16 TEG's was matched the resistance of electrical load.

Abdulsalam et al. [3] was done review on the development and various applications in the different solar ponds along with the optimization and heat extraction mode are discussed. Generally, heat can be extracted by two methods from the LCZ of the solar pond, first method is circulating hot saline water from LCZ through an external heat exchanger and this method was adopted by EI Paso solar pond. The second method, by using the heat exchanger, heat exchanger goes through the LCZ of the solar pond in closed loop. The maintenance of the solar pond can be done by several methods. The turbidity in the solar pond was controlled by using alum ($KAI(SO_4)_2.12H_2O$) because alum has a strong flocculation and also prevent the developed bacteria and algae in the solar pond. Flushing of the UCZ should be done regularly otherwise the salinity in the upper convective zone increases which affect the performance of the solar pond. They concluded that the solar pond is the best method absorbing and storage of solar energy. The salt gradient solar pond was more appropriate method to absorb the solar energy because it is low cost approach. Solar pond has several applications and performance of the solar pond was decreases with the turbidity of water,

growth of algae in the solar pond, wall shading effect etc. The plane mirror, glass cover are attached with the solar can enhance the performance of solar pond.

Kurt et al. [5] numerical and experimental analysis of the salt gradient solar pond with sodium carbonate was done. The experimental solar pond was constructed having 60 cm × 50 cm and depth of 60 cm. Eight K-type thermocouples are used for the measurement of the temperature inside the solar pond. The radiation reaches on the top surface of the solar pond by using Halogen lamps. They concluded that the density gradient of 10 % salinity can't suitable for the solar pond because the convection currents are not supressed. The minimum salinity range required for the absorption of solar energy was 12 % and temperature difference was recorded between the bottom surface and top surface of the solar pond was 12 ºC. Sodium carbonate saline water is suitable for the storage of solar energy.

Bozkurt et al. [6] was investigated the performance of the solar pond with the use of magnesium chloride as a salt and also find the energy and exergy efficiency of the solar pond. The circular solar pond having surface area 072 m^2 with the depth of 1.10 m was constructed in the Turkey. Temperature distribution inside solar pond by taking reading at several 7 points and in this solar pond salt gradient protection system was used to protect the magnesium chloride from the erosion. Energy and exergy analysed for hot storage zone i.e. LCZ and NCZ because the temperature rise only in these two zones and upper zone temperature almost equals to the ambient temperature. Results shows that the maximum and minimum average temperature of the LCZ in the solar pond was recorded 52.42 ºC for August and 24.46 ºC in November, respectively. The maximum and minimum exergy stored in the LCZ was determined as 28.84 MJ in August and 6.48 MJ for November, respectively and the maximum and minimum exergy loss in the LCZ was determined as 79.05 MJ in August and 44.84 MJ for November, respectively. The maximum exergy and energy efficiency in the LCZ was determined as 27.41 % and 26.04 % in August, respectively.

M. Karakilcik et al. [9] was investigated the temperature distribution of the salt gradient solar pond by theoretically and experimentally. This solar pond was constructed having the surface area of 4 m^2 with the depth 1.5 m in the Turkey. There are 16 temperature sensors are placed inside the solar pond. The temperature distribution of solar pond for UCZ, NCZ and LCZ was determined by modelling in two-dimensional heat balance equation and finite difference method. The various heat losses from the side and bottom surface of solar pond are function of temperature inside the solar pond. The temperature distribution was determined

by theoretically and experimentally, as shown in the Figure 2.4. the values of temperature difference between the theoretically and experimentally values in LCZ are 1.5 ºC in January, 3 ºC in May and 2.8 ºC in August.

Bozkurt et al. [10] was theoretically and experimentally investigated the performance of energy storage in the solar pond. The solar pond was studied has surface area of 2.096 m^2 and a depth of 2.0 m which was constructed in Cukurova University in Adana, Turkey. The side and bottom walls of the solar pond were insulated with glass-wool. Data logger is used to log the temperature distribution values inside the solar pond. In theoretical study, a mathematical model was developed on the principle of finite differences. In this study various heat losses from the side walls, bottom surface and upper surface was also investigated. In the results, the theoretical values are compared with experimental values and said that values difference should be less. The highest and lowest thermal efficiency in LCZ was calculated by experimentally for salt gradient solar pond was 28.41 % for August and 10.74 % for January, respectively. Similarly, the highest and lowest thermal efficiency in LCZ was calculated by theoretically for salt gradient solar pond was 30.16 % for August and 10.74 % for January, respectively.

Dincer I. et al. [11] was theoretically developed the model for the determine the energy efficiency of a solar pond and also find the ratios of the energy efficiencies with and with considering shading effect for of the each zone of a solar pond. . This experiment work was performed in Turkey with solar pond of surface area of 2 m × 2 m and with the depth 1.5 m. To record the temperature distribution for inner zones in solar pond there are 16 temperature sensors are placed inside the zones of solar pond. Results showed that the increase the shading area of the solar pond then efficiency of the solar pond decreases. If the incident angle of coming solar radiations increases, then the solar radiations falling on the upper surface of the solar pond was decreases. The overall shading area of the LCZ, LCZ and UCZ are 1.37m^2, 0.87m^2 and 0.07m^2. The highest energy efficiencies of the solar pond with and without considering shading area inside the solar pond: 28.11% and 37.25% for the LCZ, 13.79% and 16.58% for the NCZ and 4.22% and 4.30% for the UCZ, respectively. Conclusion of this experiment: the temperature for the each distinct zones of the solar pond depend on the intensity of solar radiation incident on upper surface, thickness of different zones, shading area inside the solar pond and various heat losses from all the surface of the solar pond.

Bozkurt I. et al. [12] was theoretically investigated the performance of the solar pond due to the effect of sunny area ratios. The solar pond analysis was taken four different cases in which surface area of solar pond changes and depth of solar pond was 1.5 m and similarly four more cases with the depth of 2 m for theses solar ponds. The thickness of the UCZ, NCZ, and LCZ are 0.1m, 0.5m and 0.9 for all the cases having the surface area are 1, 4, 9, 16 m^2 and other all are similar but the thickness of LCZ was 1.4 m. The temperature inside the solar pond changes with horizontal and vertical direction, therefore 2 dimensional modeling should be done for heat losses from the wall. Results showed that the maximum and minimum sunny area in the lower convective zone for all the four cases are 33.21 %, 64.75 %, 76.50 % and 82.37 % and 3.31%, 48.35%, 65.54% and 74.31%, respectively. Therefore, we can say that it is important to select the appropriate dimensions of the solar pond for the maximum efficiency of the solar pond. The amount of the sunny area for all the zones is decreases with the depth of the solar pond. Maximum temperature of solar pond having surface area of $16m^2$ and $1m^2$ are 86.84ºC and 31.5ºC therefore it is not possible to store the energy for area of $1m^2$. They concluded that the sunny area of the solar pond was increased by increasing the surface area of the solar pond and by decreasing the depth of the solar pond.

Karakilcik M. et al. [13] was studied theoretically and experimentally on the performance of solar pond. In experimental work, the temperature distributions of the solar during the month of January, May and August was investigated. Solar pond used in this study having surface area of 4 m^2 and depth of 1.5 m. solar pond has three distinct zones and the thickness of UCZ, NCZ and LCZ were 0.1, 0.6 and 0.8m respectively. A mathematical model was theoretically developed for the determination of thermal efficiencies of UCZ, NCZ and LCZ. The solar energy is measured with the help of pyranometer. Results showed that the temperatures of the UCZ,NCZ and LCZ was observed 35.0ºC in August, 10.4ºC in January and 27.9 º C in May, 44.8ºC in August, 13.9ºC in January and 37.9 º C in May and 55.20ºC in August, 16.91ºC in January and 41.1 ºC in May respectively. The efficiencies of UCZ, NCZ and LCZ are 0.09%, 3.17% and 9.67% in January, 2.86%, 8.6% and 17.54% in May and 4.54%, 13.79% and 28.11% in August respectively. Finally, concluded that the efficiency of solar pond can be increased by decreasing the shading area of solar pond, decreases the various losses takes places from all the surfaces of the solar pond.

Bezir et al. [15] was experimental and numerical performance of the salt gradient solar pond with and without using reflector. The solar pond having the surface area of 3.5 m × 3.5 m

with the depth of 2 m was constructed. To increase the amount solar radiations on the top surface of the solar pond there are two reflector are used in such a way that at a time one reflector is fixed inclination angle and other is rotated from 0 º to 180 º to track the sun. This reflector was also used as cover during the night to reduce the thermal losses from the top surface of the solar pond. Reflector was attached with the electric motor to rotate the reflector. Also find the amount of solar radiations fall on the top surface of the solar pond by theoretically. The computational modelling was done for the solar pond with and without reflector and with reflector as a cover or without cover. The temperature distribution with reflector and cover, without reflector and with cover and without reflector and cover are determined, as shown in the Figure2.1. They concluded that the performance of the solar pond was increased by 25 % by using reflector. The effect of cover on the performance of the solar pond is negligible because temperature difference with and without cover was 1 ºC. The effect of reflector on the performance of the solar pond is significantly high because temperature difference with and without reflector was 10 ºC.

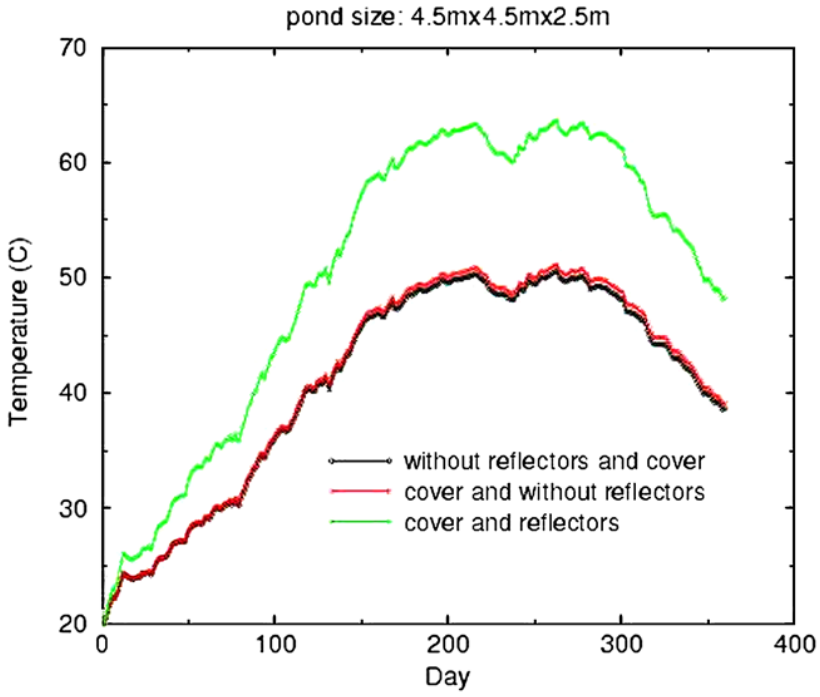

Figure 2.1 the temperature distributions in the LCZ of the solar pond with reflector and cover, without reflector and with cover and without reflector and cover (β_1 = 30º and β_2 = 89º) [15]

Bozkurt et al. [16] was done investigation of performance for the salt gradient cylindrical solar pond with three transparent covers on the top surface of the solar pond. The performance of solar pond was evaluated by using three transparent covers i.e. glass,

polycarbonate and mica cover and measuring the temperature distribution and density distributions inside the solar pond. To reduce the thermal losses from the top surface of the solar pond there are transparent cover is used and find the transmittance, reflectance and absorptance of the covers and evaluate the energy efficiency of the cylindrical solar pond. Transmission coefficient for glass, mica and polycarbonate was determined, as shown in the Figure 2.2. The results of the cylindrical solar pond are that in which highest transmission coefficients for the mica, polycarbonate and glass covers are 0.6394, 0.6411 and .6760, for the month of June, respectively. Similarly the highest reflection coefficients for the mica, polycarbonate and glass covers are 0.3115, 0.3120 and 0.3050 in December, respectively and the highest absorption coefficients for the mica, polycarbonate and glass covers are 0.0124, 0.0512 and 0.0609 in June, respectively. The highest thermal efficiency of cylindrical solar pond was determined for the glass cover; polycarbonate and mica are 17.86 %, 16.95 % and 15.86 %, respectively. Therefore, the performance of the solar has maximum by using the glass cover on the top surface of the solar pond

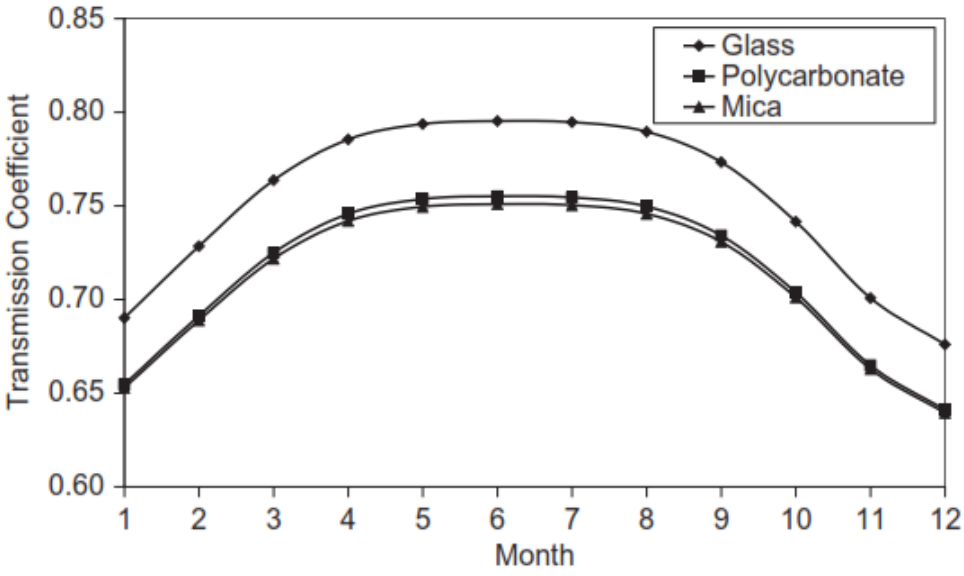

Figure 2.2 The transmission coefficient of the transparent covers [16]

Husain et al. [18] was studied experimentally of solar pond having the surface area of 2500 m^2 and depth of 1.9 m. This salt gradient solar pond was built with the help of natural brine from the Zabuye lake in Tibet. This solar pond was started for 105 days and maximum temperature measured was 39.1 ºC. Firstly, solar pond was filled with NaCl saline water up to the height of 1.4 m from bottom and then filled with fresh water by expending pipe and this

pipe continuous move in upward direction to fill the up to top of the solar pond. The gradient was developed in the solar pond by taking some time. The temperature of lower convective zone was varied from 7.5 ºC to 39.1 ºC and the increase in the average temperature of lower convective zone was increased 0.69 ºC per day. The heat loss from the walls of the solar pond was needed to analyse further in future.

Sexena A.K. el al. [19] studied the effect of various heat losses from side and bottom walls with depth of solar pond by using simulation analysis for non-insulated salt gradient solar pond. The solar pond analyzed in this study having surface area of 20 m*20 m and depth of water table was varying from 5 m to 25 m and then last takes 50 m. Results showed that the temperature of pond increases with the deeper of the water table and does not effect on time of acquiring of solar pond temperatures. Thermal performance for overall system would increase up to significant depth of the water table, if we further increase in the depth then decrease the increasing rate of thermal performance of the solar pond. There are various parameters i.e. ambient parameters, pond dimensions and soil properties can influence the significant depth of the solar pond. The maximum temperature, minimum temperature and maturation time of the solar pond is significantly depends on the dimension of the solar pond and ambient conditions but not depends on the depth of water table. Conclusion from this study was the importance of depth of the solar pond and select appropriate depth of the solar where the solar pond performance has maximum.

Dehghan et al. [20] was investigated experimentally the performance of square and circular solar pond. The square and circular solar pond both having the surface area of 3 m^2 and with the depth 1.5 m was built in Bafagh city, Iran. To measure the temperature distribution inside the solar pond there are data logger was used to record the value for 11 months after every 10 minutes. To distinguish between the performance of the square solar pond with circular solar pond energy balance model and exergy balance model was developed for all the ones inside the solar pond. Results concluded that the performance of circular solar pond was higher than the square solar pond because the temperature in the circular solar pond was higher than the square solar pond. The energy efficiency of square and circular solar was determined, as shown in the Figure 2.3. The maximum energy efficiency and exergy efficiency in LCZ of circular solar pond was determined 25.8 % and 2.44 % respectively. Similarly, the maximum energy efficiency and exergy efficiency in LCZ of square solar pond was determined 23.65 % and 1.91 % respectively.

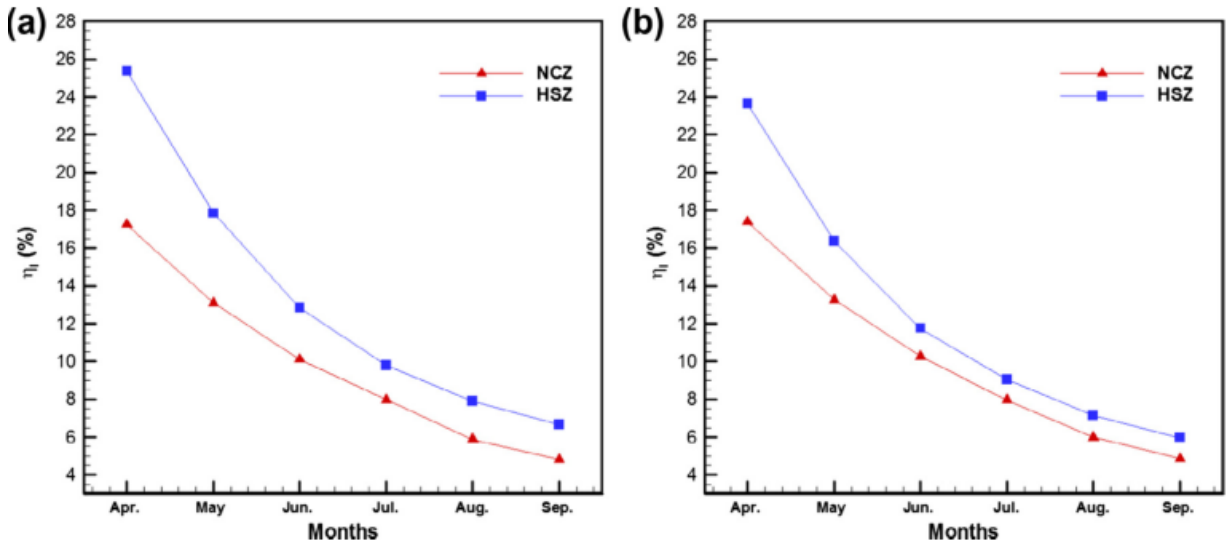

Figure 2.3 Energy efficiencies for inner zones of two solar ponds: (a) circular solar pond and (b) square solar pond. [20]

Sakhrieh A. et al. [21] was investigated both numerical and experimental part of the solar pond on April 14, 2010**.** In the numerical part, predict the temperature at various points inside the insulated salt gradient solar pond with the help of the MATLAB and in experimental method, to determine the performance of the solar pond and the solar pond was constructed at the University of Jordan having the surface area of 3.5m^2 and with depth of 1.0m and it was insulated with 5cm IZACAM insulation and the thermal conductivity of insulation is 0.034 W/mK. The temperature distribution evaluated with the help of 16 T-type thermocouples are placed in the solar pond. Results showed that as the ambient temperature increases then the temperature in the LCZ and NCZ will increases but after 12:00 pm the ambient temperature decreases while the temperature of LCZ still increases up to 5 pm and the temperature in the NCZ goes on decreases because LCZ has the tendency to absorb the heat from the coming solar radiation and NCZ decreases due to atmosphere temperature. The highest and lowest temperature in the LCZ was recorded are 46.9 ºC 39.5 ºC. The temperature of NCZ and UCZ are increases with ambient temperature and decreases with the ambient temperature deceases but temperature in the LCZ increases throughout the day.

Beniwal et al. [22] was theoretically evaluated the various heat losses from the side, top and bottom side of the salt gradient solar pond. In this analysis the solar pond insulation thickness was varied to find the effective insulation and also modeled the solar pond with and without insulation around the sides of the solar pond. There are different types of insulating materials

i.e. mica power, dry cement, dry sand, marble dust and mud power are taken in our study to check the best insulating material required for the solar pond. They concluded that the minimum in the solar pond was achieved by using the marble dust as an insulating material of thickness 0.20 m and 50 % porosity and insulation should be more effective when interstitial air pressure of insulating material are low in the range of 0.3 to 0.5 mm of mercury. All the heat losses should be decreases in this range of pressure in the insulation material.

El-Sebaii et al. [23] was done a review study on the history of the solar ponds. In this paper, they tells about the different types of the solar pond was studied and solar pond was discovered as a natural phenomenon in 19th century. Stability in the solar pond was attained by controlling the density of saline water in the pond which depends on the salinity of the liquid in the solar pond and the temperature inside the solar pond. Solar pond is large heat storage device therefore several applications of the solar pond were discussed i.e. cooling and heating of buildings, desalination, agricultural crop drying, power production, industrial process heat, green house heating etc. The review study of solar pond was concluded that the salt gradient solar ponds are more stable for long-period energy storage and without salt solar pond are more stable for the short-period energy storage. In salt less solar pond the temperature rise is rapid bit in salt gradient solar pond temperature rise is very slow as compare to other. In the shallow solar ponds, the storage performance was improved and radiation reaches to the depth of the solar was decreased by insulation the top surface of the solar pond. Temperature, salinity and density has almost same trend inside the solar pond i.e. all these are highest in the LCZ and constant throughout the LCZ and continuously decreasing towards the upper layer of the NCZ and last the temperature, salinity and density are constant in UCZ and lowest values in the LCZ.

Ramadan & Khallaf [24] was experimentally evaluated the thermal performance of the shallow solar pond with and without double glass cover and with and with and without reflector mirror during the heat extraction. The solar pond used in this study having the surface area of 1 m^2 with the depth of 0.088m. The solar pond performance was evaluated in the terms of the coefficients of heat loss. They concluded that the performance of solar pond has maximum when the solar pond is used with the double glass cover and outer mirror reflector with mirror inclination angle is continuously changes after every 30 minutes. The solar pond achieved the maximum temperature of 60 ºC under the heat extraction and 88 Kg of heated water was obtained. If the mass flow rate through the heat exchanger is large then

the outlet temperature of fluid through heat exchange was found to be decreases. In the shallow solar ponds, the storage performance was improved decreased by insulation the top surface of the solar pond and solar radiations reaches to the depth of the solar pond was decreases by insulation the upper surface of the solar pond.

Kumar & Kishore [25] was built a large solar pond having surface area of 6000 m^2 in Bhuj, India and the heat of this solar pond was used for the pasteurisation of milk dairy plant. There are different types lining schemes are studied and lining scheme was made up of clay with LDPE (low density polyethylene). In this study, algae was controlled by using bleaching power and liquid chlorine initially but this was method was not suitable then they used hydrochloric acid and sulphuric acid to make clarity of water. Diffuser was used to establish proper gradient zone in the solar pond and it depends on the various parameters i.e. diffuser diameter, salinity values that need for equilibrium, width of the diffuser, geometry of the solar pond and Froude number. This resulted that the Froude number should be maintained at 18 and the maximum temperature attained in this solar pond was at 99.8 ºC. The solar pond was designed in such a manner that supply the 80 m^3 of hot water per day and the temperature of the water should be at 70 ºC. They concluded that the hot water was spilled to milk dairy plant and this plant save the 935 MT of lignite per year and payback period was determined as less than five years and 7,00,000 rs. of amount was saved through this solar pond heat by milk plant.

Hongsheng et al. [26] experimental investigation of trapezoidal salt gradient solar pond and simulation was done to check the performance of the solar pond. The solar pond has been constructed having top surface area of 2.4 m × 2.4 m and bottom surface area 1 m × 1 m and with the depth of 1.2 m. Soil is used for the insulating the side walls of the solar pond. The amount of solar intensity on the surface of the solar pond and the temperature of the solar was recorded experimentally and it compared with the simulated results. From the simulation, compare the temperature distribution of the rectangular solar pond and trapezoidal solar pond and concluded that trapezoidal solar pond has higher temperature then rectangular solar pond temperature by the difference of 5 ºC. The trapezoidal solar pond and the highest temperature was recorded was 51.2 ºC. The temperature distribution was evaluated by simulation, as shown in the Figure 2.5.

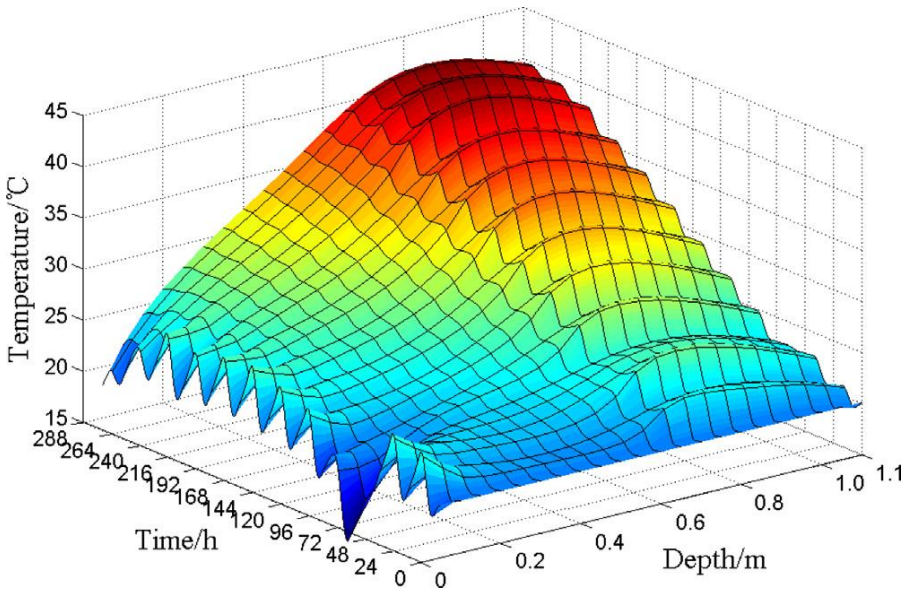

Figure 2.4 The temperature distribution cloud solar pond [26]

Chapter 3

Experimental setup and procedure

3.1 Description of experimental

The main aim of experimental setup is to develop a trapezoidal salt gradient solar pond. Figure 3.1 shows the snapshot of trapezoidal salt gradient solar pond (TSGSP) used in the present study. The solar pond having a top surface area of $1.625 \times 1.625\,m^2$ and bottom surface area of $0.71 \times 0.71\,m^2$ and depth of 0.97 m was constructed at Thapar University in Patiala, India (30.3568° N latitude, 76.3688° E longitude). The bottom and side walls of the pond were made of iron sheets of 3 mm thickness. The bottom and side walls of the solar pond were covered with the insulation consisting of glass-wool of thickness 150 mm and this insulation is covered with polycarbonate sheets of thickness 1 mm. The inner and outer walls of a solar pond were painted with anti-corrosion paint (red-oxide) to avoid corrosion and then painted with black paint (rough black board paint) to absorb maximum solar radiations. The saline water used in the present study was prepared by dissolving the NaCl salt into fresh water. Neat about 180 Kg NaCl is consumed for preparing saline water in the solar pond.

Firstly, the solar pond was filled with the saline water, having concentration of 20 % by wt., up to the height of 0.45 m from bottom to form lower convective zone (LCZ) of solar pond. Then the solar pond was filled with the saline water with continuous decreasing concentration up to height of 0.35 m from upper layer of LCZ to create non-convective zone (NCZ). Finally, the solar pond was filled with fresh water up to a height of 0.10 m to form upper convective zone (UCZ) because the density and concentration of water in the UCZ is t almost near to the density and concentration of fresh water. The top surface of the solar pond was covered with two transparent glass covers placed at a gap of 10 mm and the thickness of each glass cover was 5 mm. The double glass is first framed in the structure then place on the top surface of the solar and transmittance of solar radiation through glass is 0.89. A reflector made of aluminium sheet of thickness 0.5 mm was used for enhancing the solar radiations on the top surface of a solar pond. The surface area of reflector was equal to the top surface area of the solar pond. The back-side of the reflector was covered with the glass-wool insulation of thickness of 70 mm so that insulated reflector can be used as cover on the top surface of solar pond to reduce the thermal losses i.e. convection losses during night.

Figure 3.1 shows the snapshot of trapezoidal salt gradient solar pond (TSGSP)

The reflector is kept at an angle at which the reflector reflects the maximum amount of solar radiation on the top surface of the solar pond. In order to receive the maximum solar radiation on the reflector surface throughout the day, the reflector is positioned east facing during 9 am to 11 am, south facing during 11 am to 2 pm and west facing during 2 pm to 5 pm. The temperature distribution of UCZ, NCZ and LCZ has been measured for the trapezoidal solar pond with and without double glass cover. As the temperature of water increases in upper convective zone therefore, concentrated salt water rises to the surface of solar pond. To remove this water from upper zone flushing water takes place in the pond, in which continuous water comes out through the outlet port and saline water goes inside through inlet port in the bottom side. Water come out from the top surface of solar pond was collected in tray for further use of use of salt. Water in the tray was evaporated and salt is left in the tray, further this salt is used for dissolving it in water for increase the density of water in bottom zone.

3.2 Fabrication of trapezoidal salt gradient solar pond

Various steps acquired for the fabrication of trapezoidal salt gradient solar pond. In this section solar pond is fabricated accordingly as discussed in the section 3.1. Figure 3.2 shows the various steps involved in the fabrication of the trapezoidal salt gradient solar pond. First of all, MS (Iron sheet)sheet having the thickness of 3 mm was cut into five pieces in which four pieces are of same size which is the side walls of the solar pond and fifth piece having the dimensions of the base of the solar pond i.e. 0.71×0.71 m^2. Then these pieces were welded and basic structure of solar pond is become complete as shown in Figure 3.2 (a). The bottom and side walls of the pond were made of iron sheets of 3 mm thickness. The inner and outer walls of a solar pond were painted with anti-corrosion paint (red-oxide) to avoid corrosion. To absorb maximum solar radiations coming from the sun solar pond was painted with black paint (rough black board paint) because only black colour absorb the solar radiations and absorption coefficient of black painted was maximum. Black colour silicon was also used for the reduction of corrosion; therefore 1 mm thickness of silicon was paste on the inner walls of solar pond. The top view solar pond painted black colour was shown in the Figure 3.2 (b).

Figure 3.2 (a)

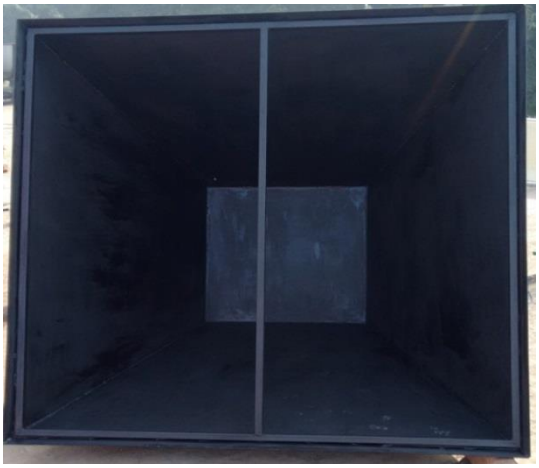

Figure 3.2 (b)

An internal brick structure was made with surface area of 0.71×0.71 m^2 and outer brick structure of surface area of 1.13×1.13 m^2. The internal brick structure was filled with the rock-wool for insulating the bottom surface of the solar pond and gap between the internal and outer surface was also filled with insulation. Then this solar pond was placed on

Figure 3.2 (c)

the brick structure having area of 0.71×0.71 m^2 as shown in the Figure 3.2 (c). Sheathing is required for the insulation of side walls of the solar pond. Sheathing was made with the polycarbonate sheet having thickness of 1 mm and side edges of sheathing were supported with the stainless steel. After sheathing of solar pond, side walls were filled with rock wool for insulation of 150 mm thickness.

Figure 3.2 (d)

The solar pond with proper insulation and sheathing was shown in the Figure 3.2 (d). Five connections were made in the solar pond for various purposes. Top two connections required for the flushing out saline water and input fresh water, bottom connection for drainage of water, other two is used for the heat exchanger used for further applications. Basic structure of solar pond was made with proper insulation and connections. To measure the temperature distribution inside the solar pond eight T-type thermocouples was used at different height and this all thermocouples were coupled with stainless-steel frame as shown in the Figure 3.2 (e). T-type thermocouples were placed at eight specific locations i.e. at a height of 0.01, 0.13, 0.25, 0.37, 0.49, 0.61, 0.73 and 0.85 m from the bottom of solar pond.

Figure 3.2 (e)

Figure 3.2 (f)

Solar pond has three distinct zones was discussed in the introduction chapter. Thickness of LCZ, NCZ and UCZ are 0.45, 0.35 and .10 m. Therefore three marks were drawing in the solar pond to see the height of

different zones. Salt was dissolved in the fresh water with help of washing machine to prepare saline water. Washing machine was properly dissolving the salt in the water in less time. The solar pond is filled with saline water having concentration of salt 20% by wt. up to the upper layer of LCZ, and then salinity of saline water is continuously decreasing up to the UCZ and UCZ zone is filled with fresh water. The solar pond was filled with saline water as shown in Fig 3.2 (g).

Figure 3.2 (g)

The solar pond was covered with double glass cover to reduce the top losses i.e. convective and evaporative losses from the top surface of the solar pond. First of all wooden frame was built where the double glass was placed. Wooden fame was made for top surface of solar pons as shown in the Figure 3.2 (h).

Figure 3.2 (h)

Double glass cover having the top surface area equals to the top surface of solar pond. The thickness of each glass was 5 mm. Double glass cover was tempered for safety purpose and double glass cover was made in four pieces because the surface area of top surface has large. Two glasses was placed on the wooden that act as lower glass cover, as shown in the Figure 3.2 (i). The upper glass cover was placed in such was that gap between the top and bottom glass was maintained at 10 mm. Silicone sealant is used for the proper sealing of lower glass

Figure 3.2 (i)

cover with wooden frame. The solar pond with double glass covers as shown in the Figure 3.2 (j). Transmittance of transparent glass has the value of 0.89. Two T-type thermocouples was placed inner and outer side of glass cover to measure the temperature of the bottom and top glass of solar pond. Assembly of trapezoidal salt gradient solar pond with double glass cover has been completed.

Figure 3.2 (i)

This double glass covered TSGSP coupled with the reflector. The reflector was made up of aluminium sheet. This aluminium sheet was cover with the insulation of thickness 70 mm and insulation was supported with the help of galvanised iron sheet if thickness 1 mm. Therefore, insulated reflector also used as a cover during night to reduce the thermal losses. Firstly, reflector stand was built with square pipe as shown in the Figure 3.2 (j). The reflector made up of aluminium sheet and insulted with rock-wool which is covered with the galvanised sheet as shown in the figure 3.2 (k).

Figure 3.2 (j)

In this study, Reflector is used with changes its inclination angle and changes its position to track the sun, for collecting maximum solar radiation on the top surface of solar pond. The solar pond with the double glass coupled with reflector is shown in the figure 3.2 (l).

Figure 3.2 (k)

Figure 3.2 (k)

Figure 3.2 Fabrication of TSGSP with double glass and coupled with reflector

3.3 Instrumentation and measurement

To measure the temperature distribution inside the solar pond and to measure temperature of upper glass cover and lower glass cover, there are 10 T-type thermocouples are placed inside solar pond. T-type thermocouple is made up of copper and constantan and it is very stable thermocouple which regularly used for low temperature applications. T-type thermocouples are used in this study having the accuracy of ± 1.0 °C and range of thermocouple is -270 °C to 200 °C. Eight T-type couple are used to measure the temperature of UCZ, NCZ and LCZ in solar pond and placed in such way that distance between each of them are equal. Firstly L-shape stainless steel frame was made because solar pond contains saline water which causes corrosion, to prevent from corrosion and to support the thermocouples frame is made up of stainless steel. First thermocouple was placed at distance 1 cm from the bottom surface of solar pond. Next all the thermocouples are placed one by one at 12 mm gap. Locations of eight thermocouples are at a height of 0.01, 0.13, 0.25, 0.37, 0.49, 0.61, 0.73 and 0.85 m from the bottom of solar pond as shown in the Figure 3.3. The

bottom part of stainless steel frame is fixed with the bottom side of the solar pond with the help of silicon sealant and upper part of stainless steel is fixed with the upper part of solar pond. Theses all the thermocouple are attached with the thermocouple extension wire of length 9 m because data logger which log the value of temperatures are fixed at distance 9 m. Data logger is further connected to the computer to get the temperature values in the solar pond.

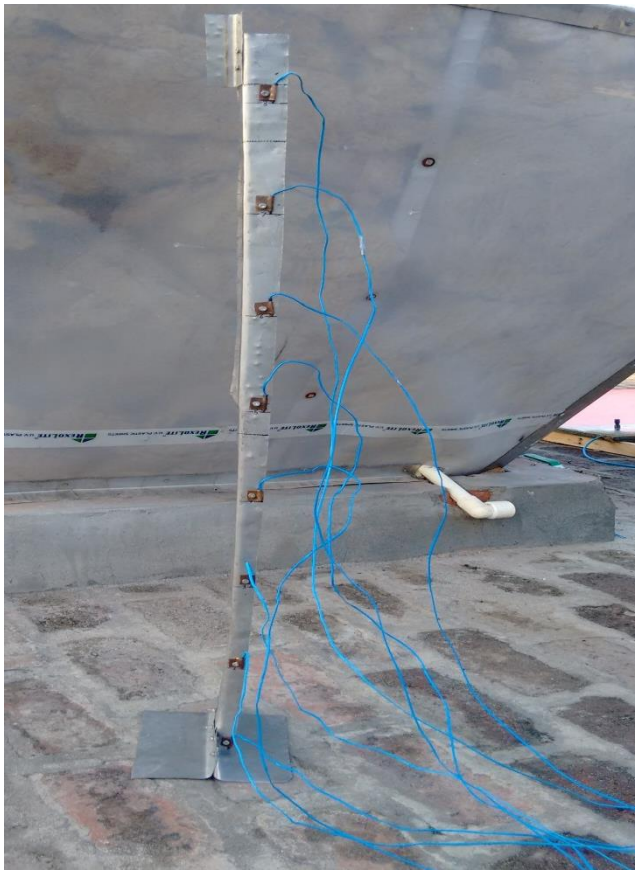

Figure 3.3 Eight T-type thermocouples with stainless steel frame

Density of saline water is measured by normal method. Take 100 ml of saline water in measuring beaker and weight the beaker from where we get density of saline water. In this work, density of three samples takes place for the LCZ, NCZ and UCZ water.

The intensity of solar radiations is measured with the help of Pyranometer. Pyranometer measures the direct solar beam and diffused radiations coming from the sun. This pyranometer takes the reading after every 10 minutes and data logger is attached which is further connected to the computer to log the values of solar intensity. The pyranometer by Kipp & Zonen (CMP 11) is used with operational irradiance 4000 W/m^2, Operating and storage temperature range -40 °C to +80 °C, and Sensitivity 7 to 14 $\mu V/W/m^2$. Solar irradiance values measured at 40 ° from the horizontal, as shown in the

Figure 3.4 shows the pyranometer

Figure 3.4, because it was fixed to this position. Convert this measured solar irradiance on the horizontal surface of solar pond by using conversion factor.

Hand-refractrometer, was used to measure the salinity of water on the principle of refraction of light. First of all put 2-3 drops of distilled water on the measuring surface of hand held refractrometer and look through eyepiece and calibrate the reading to zero where contrast line i.e. difference between dark and light line. Similarly, put 2-3 drops of sample (saline water) on the measuring surface of hand held refractrometer and look through eyepiece and note the reading where contrast was seen.

Chapter 4

Theoretical Analysis

In this section, theoretical assessment of shading area of various solar ponds was analysed. The reflector coupled with solar and should be at proper inclination angle to harvesting of solar radiation on the top surface of the solar pond. Therefore optimum inclination angle of reflector was theoretically calculated.

4.1 Shading area assessment

In this section, the shading area for the different zones of the TSGSP with and without double glass cover is determined and analysed. The shading area of square solar pond is also evaluated in order to compare the shading area of TSGSP with that of square solar pond. Three different cases of square solar ponds are considered for the purpose of comparison. These three cases of square solar pond are: the same surface area and volume, the same height and surface area and the same height and volume as that of TSGSP.

The shading length of inner zones of solar pond is shown in Figure 4.1. The shading area analysis is done by dividing the solar pond height into 30 layers, each having a thickness of 0.03 m. Therefore, UCZ has two layers i.e. 1-2, NCZ has 12 layers from 3 to14, and LCZ has 15 layers from 15 to 30.

The angle of refraction, as the sun rays passes through air to glass cover, is calculated by Snell' law as:

$$\theta_{rf1} = \sin^{-1}[(2/3)\sin\theta_i] \tag{4.1}$$

Similarly, θ_i the angle of refraction, as the sun rays passes through air to water, is determined as given below:

$$\theta_{rf2} = \sin^{-1}[(1/1.33)\sin\theta_i] \tag{4.2}$$

where θ_i is the incidence angle. The incidence angle is equal to the zenith angle which is defined as:

$$\theta_z = \cos^{-1}[\cos(\delta_d)\cos(\varphi)\cos(\theta_h) + \sin(\delta_d)\sin(\varphi)] \quad (4.3)$$

where δ_d is declination angle, φ is latitude angle, θ_h is hour angle.

The declination angle (δ_d) is defined as:

$$\delta_d = 23.45\left(\frac{360(284+n)}{360.25}\right) \quad (4.4)$$

where n is the day of the year.

Hour angle (θ_h) is defined in degrees as:

$$\theta_h = (h-12)15 \quad (4.5)$$

where h is the local solar time, $1 \leq h \leq 24$.

The shading length (Sh_I) of the I[th] layer in the TSGSP without double glass cover is evaluated as:

$$Sh_I = \{(\delta + (I-1)\Delta x)\tan\theta_{rf2} - S_I\} + (0.02\tan\theta_z) \quad (4.6)$$

where δ is the thickness where long wavelength solar radiation is absorbed, Δx is thickness of each layer i.e. 0.03 m, S_I as shown in Figure 4.1, is the horizontal distance between normal and the side surface of solar pond at i[th] layer.

The shading length (Sh_I) of the I[th] layer in the TSGSP with double glass cover is estimated as:

$$Sh_I = \{(\delta + (I-1)\Delta x)\tan\theta_{rf2} - S_I\} + [0.01(\tan\theta_z) + \tan\theta_{rf1}] \quad (4.7)$$

The shading area (A_{sh}) of the TSGSP with or without double glass cover is calculated as:

$$A_{sh} = Sh_I L_{WI} \quad (4.8)$$

where L_{WI} is the width of TSGSP at i[th] layer of solar pond.

The shading area (A_{sh}) of the I[th] layer in all the three cases of the square solar pond is evaluated as[11]:

$$A_{sh} = Sh_I L_W = (\delta + (I-1)\Delta x)L_W \quad (4.9)$$

where $A_{sh}$is the shading area of square solar pond, L_W is width of the square solar pond, Δx is thickness of each layer and Sh_l is the shading length of square solar pond.

The sunny area ratio (%) of the solar pond is calculated as [12]:

$$\text{Sunny area ratio} = \frac{A_{su}}{A_{sur}} \tag{4.10}$$

where A_{su} is sunny area of solar pond and A_{sur} is surface area of solar pond

$$A_{su} = A_{sur} - A_{sh} \tag{4.11}$$

The shading area of various solar ponds was evaluated with the help of MATLAB software. All the programs using MATLAB for the various solar ponds are written in the appendix 1, appendix 2, appendix 3, appendix 4 and appendix 5. The shading area of UCZ was determined by taking average of layers included in the UCZ. Similarly, the shading area of NCZ and LCZ was determined by taking average of layers included in the corresponding NCZ and LCZ, respectively. In our analysis of shading area, shading was calculated from 9 am to 5 pm for particular day.

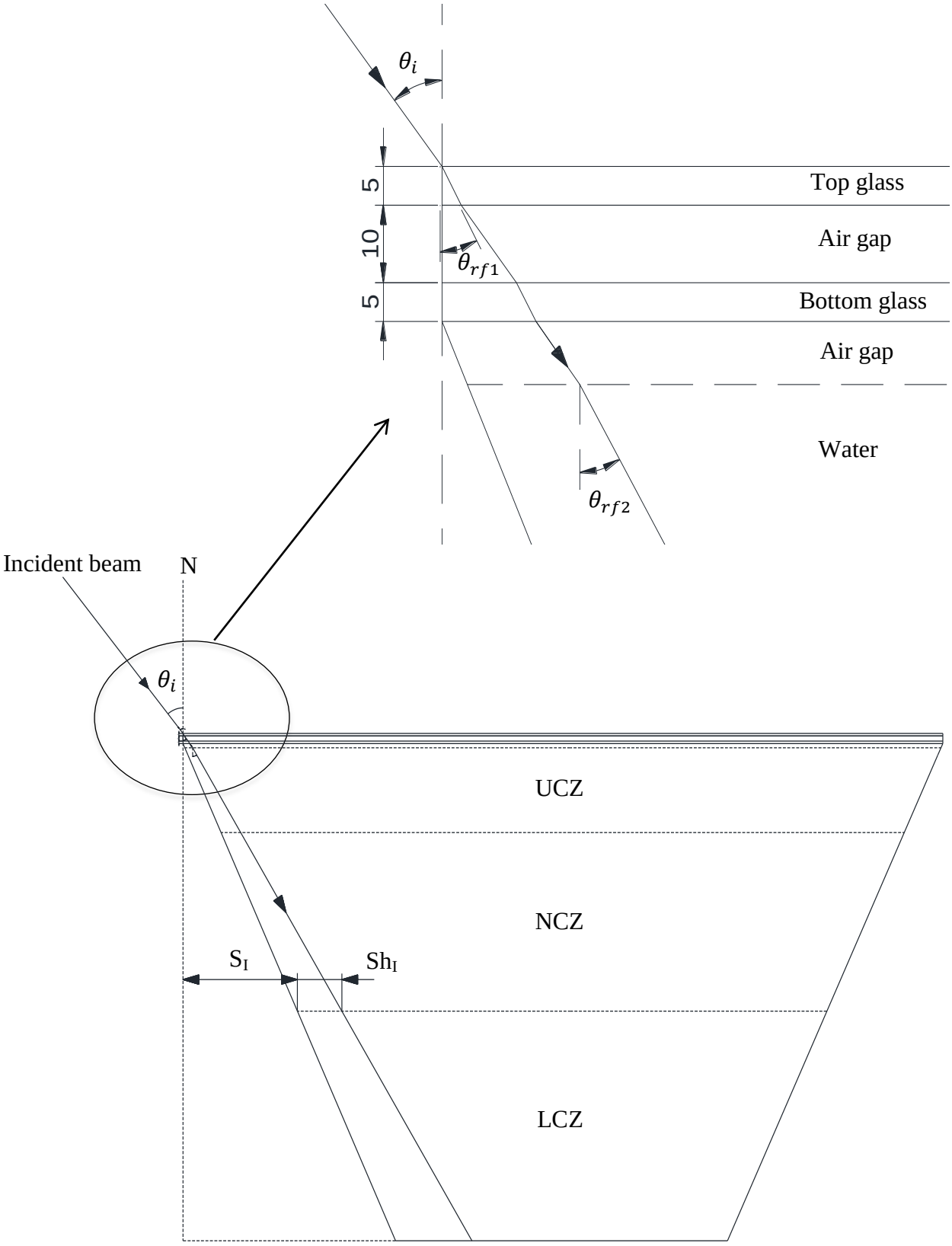

Figure 4.1 shading length of I^{th} layer in trapezoidal solar pond with double glass

4.2 Optimum angle of reflector

The performance of solar pond can be increased by using reflector which enhances the solar intensity on the top surface of solar pond. The reflector should be inclined at an optimum angle at which it reflects the maximum possible amount of solar radiation on the top surface of the solar pond. If the solar radiations reflected from the top edge of reflector enter the solar pond, then all the solar radiations reflected from the reflector will pass through top surface of solar pond. Therefore, the analysis to determine the optimum inclination angle of reflector is based on the above mentioned concept. The directions of incident and reflected solar radiations from reflector surface, as shown in Fig 4.2, are used to derive equations to determine optimum inclination angle of reflector.

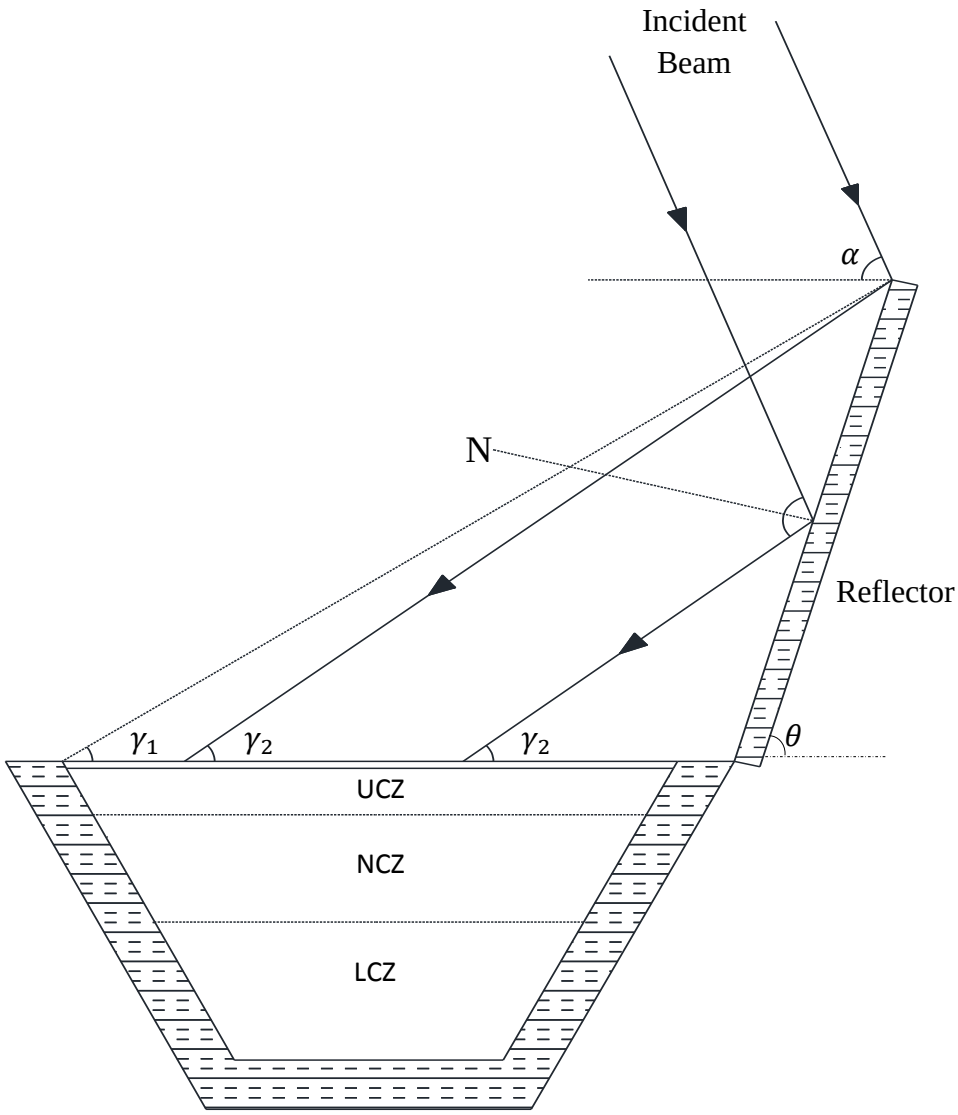

Figure 4.2 Incident and reflected solar radiations from reflector

Let us consider the reflector is inclined at an angle of θ with the horizontal surface of solar pond. The line joining the top edge of reflector and extreme end point of solar pond make an angle of γ_1 with the horizontal surface of solar pond with the inclination angle of reflector and it is calculated as:

$$\gamma_1 = \frac{l \sin\theta}{l + l \cos\theta} \tag{4.12}$$

where l the reflector length and l is is also equals to the top length of solar pond

The solar radiations make an angle α with the horizontal surface. This angle is also known as elevation angle and it is calculated as:

$$\alpha = 90° - \varphi + \delta_d \tag{4.13}$$

where φ is latitude angle, δ_d is declination angle in degrees.

Declination angle (δ_d) was calculated by using the Eq. 4 and latitude angle(φ) was already mentioned above for the location of the system. The angle between the reflected solar rays and horizontal surface of the solar pond is denoted as γ_2. The expression for γ_2 can be obtained by using the geometry as given in Fig 4.2 and it is expressed as:

$$\gamma_2 = 2\theta + \alpha - 180° \tag{4.14}$$

It is quite clear from Fig 4.2 that the reflector will reflect maximum amount of solar radiation on the top surface of the solar pond when γ_2 becomes equal to γ_1. On a particular day, the elevation angle (α) remains same throughout the day, therefore the angles $\gamma_1$and γ_2, as given by Eqs. (12) & (14), becomes only a function of reflector inclination angle (θ). Therefore, to obtain optimum reflector inclination angle, the reflector inclination angle is varied in such a way that γ_2 becomes equal to γ_1.

Furthermore, in order to receive the maximum solar radiation on the reflector surface throughout the day, the reflector is positioned east facing during 9 am to 11 am, south facing during 11 am to 2 pm and west facing during 2 pm to 5 pm, as shown in the Figure 4.3. The position of reflector changes three times by manually during the day time. To reduce the losses from the top surface of solar pond, reflector is used as a cover during night.

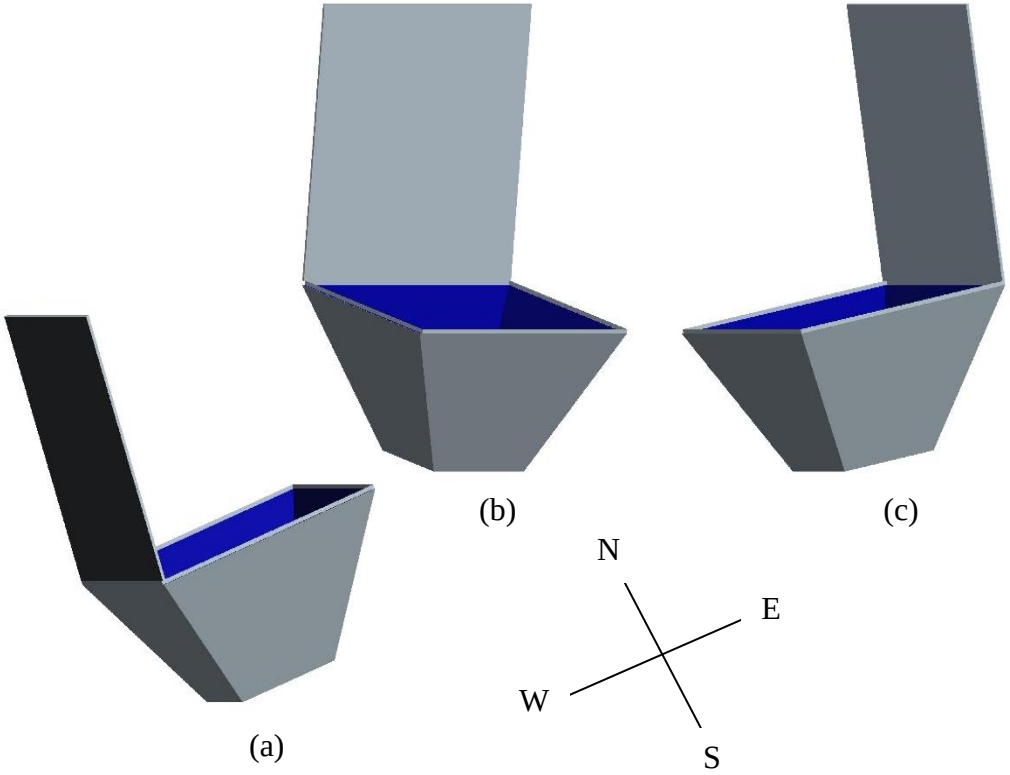

Figure 4.3 Position of reflector (a) east facing during 9 am to 11 am (b) south facing during 11 am to 2 pm (c) west facing during 2 pm to 5 pm

4.3 Energy analysis

To understand the thermal performance of solar pond, it is necessary to evaluate the thermal efficiency of solar pond. The temperature values as obtained from experiments are used to calculate thermal efficiencies of each of the three zones of TSGSP.

4.3.1 Energy analysis for UCZ

The thermal efficiency of upper convective is defined as the ratio of heat stored in UCZ to the total heat entering the UCZ and it is expressed as[20]:

$$\eta_{UCZ} = \frac{E_{Stored}}{E_{in}} = \frac{\rho_{UCZ} V_{UCZ} C_{P,UCZ} (T_{f,UCZ} - T_{i,UCZ})}{Q_{UCZ,Solar} + Q_{NCZ,UCZ}} \quad (4.15)$$

where ρ_{UCZ} is density of UCZ, V_{UCZ} is the volume of UCZ, $C_{P,UCZ}$ is specific heat capacity of UCZ, $Q_{UCZ,Solar}$ is the net amount of incident solar radiation absorbed by the UCZ, $Q_{NCZ,UCZ}$

is the heat transfer from the NCZ to UCZ through conduction, $T_{i,UCZ}$ is the initial temperature of UCZ, $T_{f,UCZ}$ is the final temperature of UCZ.

The average specific heat capacity (C_P) of the saline water in Eq. (4.15) is calculated by using an empirical equation as given below [12]:

$$C_P = (-0.0044\mathrm{s} + 4.1569)1000 \tag{4.16}$$

where s is salinity (g/kg) which is calculated by using the following equation [12]:

$$s = \frac{\rho - 998.24}{0.756} \tag{4.17}$$

where ρ is the density of saline water (Kg/m^3) in distinct zones of solar pond.

The net incident solar radiation (Q_{Solar}) absorbed by a given zone in Eq. (4.15) is estimated as:

$$Q_{Solar} = \beta E(1-\tau)A_{sur} \tag{4.18}$$

where E is solar intensity per unit area on the top surface of solar pond, β is the fraction of radiation that enters in the solar pond and it is defined as [11]:

$$\beta = 1 - 0.6\left[\frac{\sin\theta_i - \sin\theta_{rf2}}{\sin\theta_i + \sin\theta_{rf2}}\right]^2 - 0.4\left[\frac{\tan\theta_i - \tan\theta_{rf2}}{\tan\theta_i + \tan\theta_{rf2}}\right]^2 \tag{4.19}$$

and τ is the transmission function which gives the fraction of solar radiation reaching to the depth x of the solar pond and it is given by Bryant and Colbeck [27] as:

$$\tau = 0.36 - 0.08\ln(x) \tag{4.20}$$

where, x is the depth of water in metres.

The heat transfer from the NCZ to UCZ, $Q_{NCZ,UCZ}$, through conduction in Eq. (4.15) is calculated as:

$$Q_{NCZ,UCZ} = \frac{kA_{sur}}{\Delta Z_{UCZ}}(T_{NCZ} - T_{UCZ})$$

where k is the thermal conductivity of saline water, which is calculated as [28]

$$k = 0.5553 - 0.0000813C + 0.0008\,(T - 20) \quad (4.21)$$

where $C\ is\ concentration\ in\ kg/m3$ and $T\ is\ temperature\ in\ °C$.

and ΔZ_{UCZ} is the thickness of UCZ, T_{NCZ} is the temperature of NCZ and T_{UCZ} is the temperature of UCZ.

4.3.2 Energy analysis for NCZ

The thermal efficiency of NCZ is calculated as:

$$\eta_{NCZ} = \frac{E_{Stored}}{E_{in}} = \frac{\rho_{NCZ} V_{NCZ} C_{P,NCZ} (T_{f,NCZ} - T_{i,NCZ})}{Q_{NCZ,Solar} + Q_{LCZ,NCZ}} \quad (4.22)$$

where ρ_{NCZ} is density of NCZ, V_{NCZ} is the volume of NCZ, $C_{P,NCZ}$ is specific heat capacity of NCZ, $Q_{NCZ,Solar}$ is the net incident solar radiation absorbed by the NCZ, $Q_{LCZ,NCZ}$ is the heat transfer from the LCZ to NCZ through conduction, $T_{i,NCZ}$ is the initial temperature of NCZ, $T_{f,NCZ}$ is the final temperature of NCZ

The heat transfer from the LCZ to NCZ, $Q_{LCZ,NCZ}$, through conduction in above equation is calculated as:

$$Q_{LCZ,NCZ} = \frac{kA_{sur}}{\Delta Z_{LCZ}} (T_{LCZ} - T_{NCZ})$$

4.3.3 Energy analysis for LCZ

The thermal efficiency of LCZ is calculated as:

$$\eta_{LCZ} = \frac{E_{Stored}}{E_{in}} = \frac{\rho_{LCZ} V_{LCZ} C_{P,LCZ} (T_{f,LCZ} - T_{i,LCZ})}{Q_{LCZ,Solar}} \quad (4.23)$$

where ρ_{LCZ} is density of LCZ, V_{LCZ} is the volume of LCZ, $C_{P,LCZ}$ is specific heat capacity of LCZ, $Q_{LCZ,Solar}$ is the net incident solar radiation absorbed by the LCZ, $T_{i,LCZ}$ is the initial temperature of LCZ, $T_{f,LCZ}$ is the final temperature of LCZ

Chapter 5

Results and discussions

The month-wise sunny area ratio of trapezoidal and square solar ponds are shown in Figure 5.1. The figure shows that the sunny area ratio for trapezoidal solar pond with double glass cover is always higher than the other various solar ponds studied in this work. The highest sunny area ratio (%) for trapezoidal solar pond with and without double glass cover is 94.12% and 93.65% respectively, and the highest sunny area ratio for square solar ponds with the same surface area and volume, with the same surface area and height and with the same height and volume as that of trapezoidal solar pond are 88.86%, 84.2% and 78.6% respectively in the month of June, 2016. It can also be observed from the figure that the sunny area ratio is maximum in the month of June due to minimum incident angle in this month and the sunny ratio is minimum in the month of December due maximum incident angle in this month

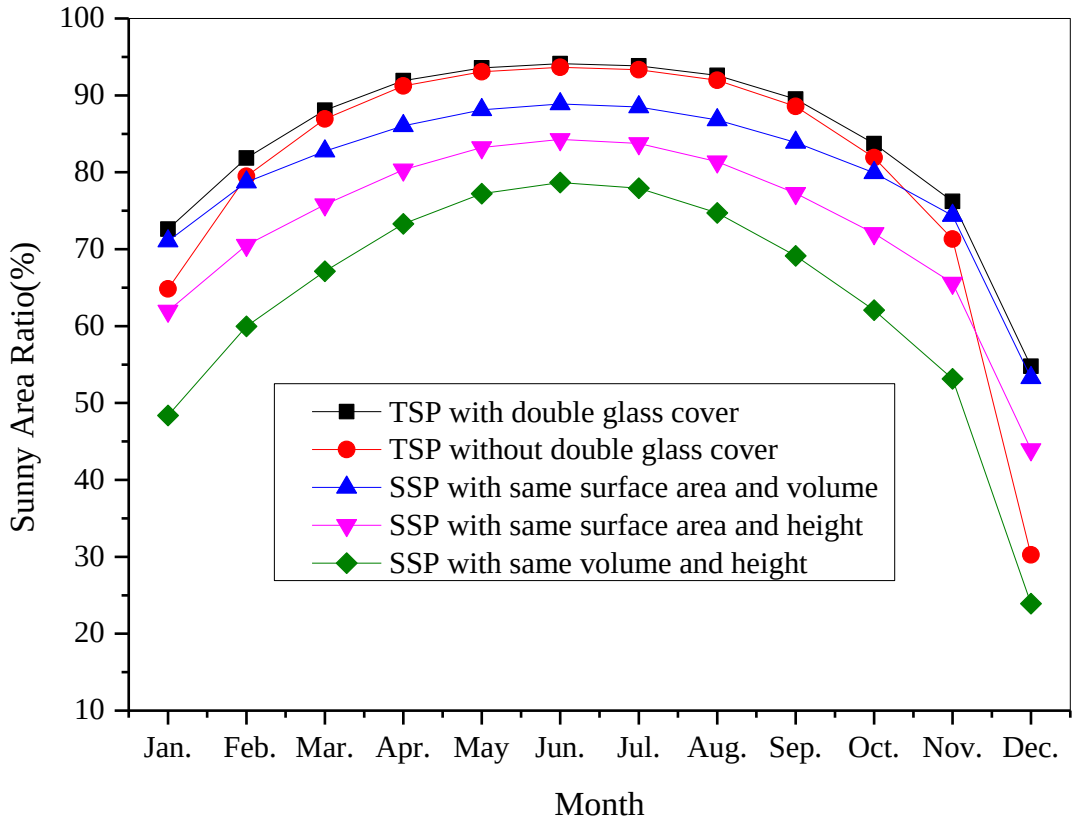

Fig 5.1 Comparison of sunny area ratio (%) for the various solar ponds

Figure 5.2 shows the yearly variation of shading area of UCZ of the various solar ponds studied in this work. The figure shows that the shading area of trapezoidal solar pond with double glass cover is always lower than that of other solar ponds studied in the work. The reason is that the surface area in trapezoidal solar pond continuously decreases from top to bottom. The yearly average shading area in UCZ of trapezoidal solar pond is 0.119 m^2. The yearly average shading area in UCZ is found to be maximum for square solar pond having the same surface area and height as that of trapezoidal solar pond and the value of shading area for this solar pond is 0.259 m^2. Square solar with same volume and height having less shading area because surface area value is less as compared to other two square solar ponds.

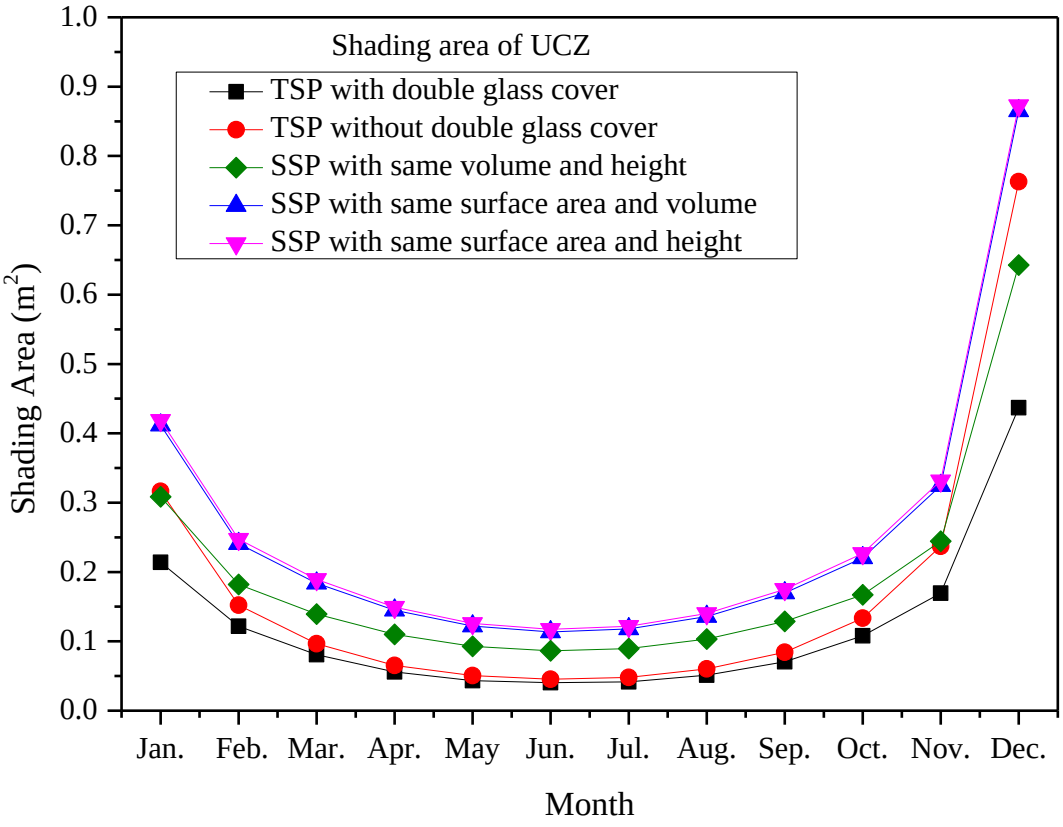

Fig 5.2 Comparison of the shading area of UCZ for various solar ponds

Figure 5.3 and Figure 5.4 show the variation of the shading area of NCZ and LCZ of the various solar ponds during the year. Figure 5.3 reveals that the lowest shading area in NCZ for trapezoidal solar pond with and without double glass cover is 0.086 m^2 and 0.092 m^2 respectively, and the lowest shading area in NCZ for square solar ponds with the same surface area and volume, with the same surface area and height and with the same volume

and height as that of trapezoidal solar pond are 0.202 m^2, 0.272 m^2 and 0.20 m^2 respectively in the month of June, 2016. The shading area difference between the square solar pond with same surface area and volume and same surface area and height was increases because in the square solar pond with same surface area and volume and height is less and in NCZ height plays significant role in shading area of solar pond.

It can be seen from Figure 5.4 that the lowest shading area in LCZ for trapezoidal solar pond with and without double glass cover is 0.282 m^2 and 0.288 m^2 respectively, and the lowest shading area in LCZ for square solar ponds with the same surface area and volume, with the same surface area and height and with the same volume and height as that of trapezoidal solar pond are 0.385 m^2, 0.580 m^2 and 0.427 m^2 respectively in the month of June, 2016. The comparison of shading area in NCZ and LCZ reveals that the effect of shape and configuration of solar ponds is most significant in LCZ because LCZ is the bottom zone of solar pond. The square solar pond with same surface area and volume has lowest shading area as compared to other two square solar ponds because LCZ is bottom most zone surface area increases with the depth and height the square solar pond with same surface area and volume is near about half of the height of other two square solar ponds .

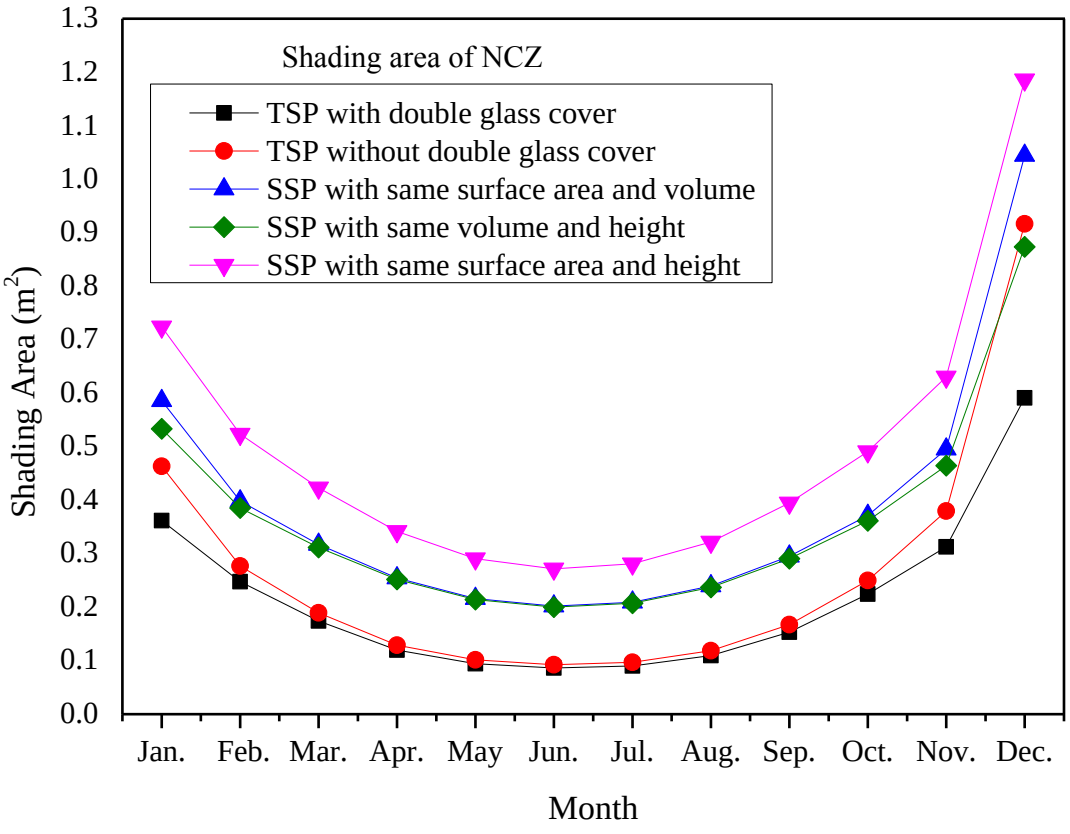

Fig 5.3 Comparison of the shading area of NCZ for various solar ponds

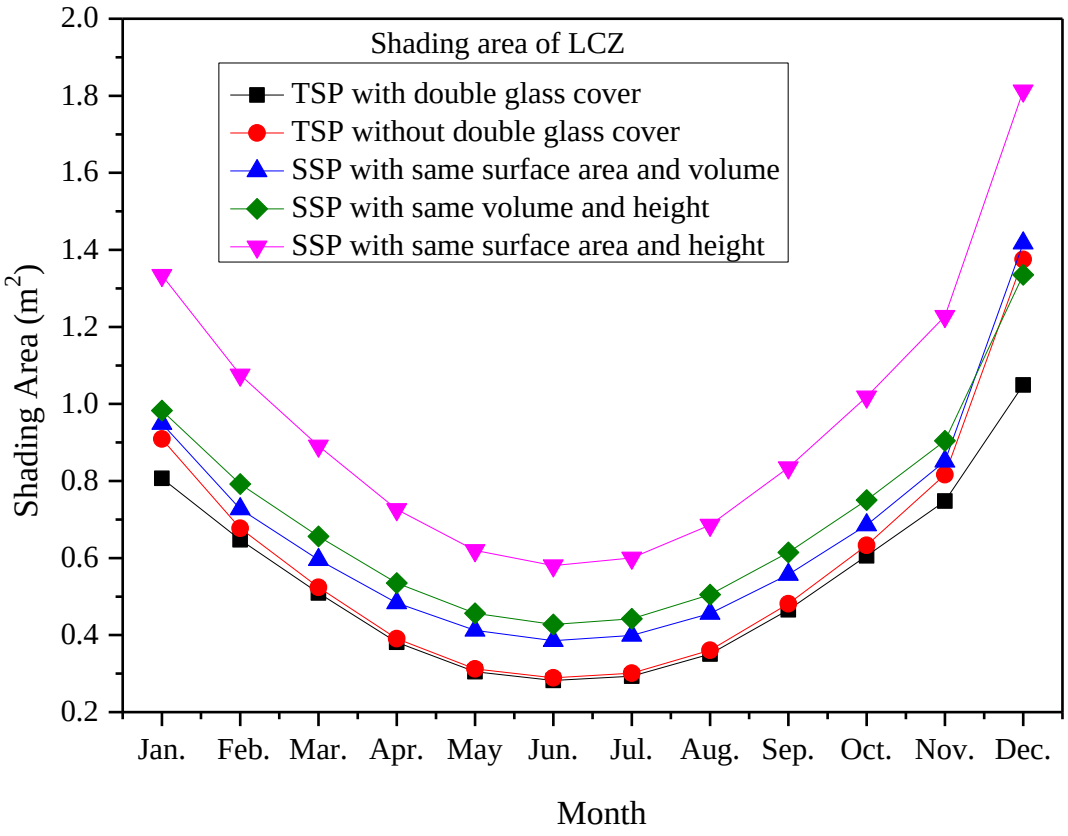

Fig 5.4 Comparison of the shading area of LCZ for various solar ponds

Fig 5.5 shows the comparison of the average shading area for various solar ponds. The lowest shading area in trapezoidal solar pond with and without double glass cover is 0.078 m^2 and 0.084 m^2 respectively, and the lowest shading area for square solar ponds with the same surface area and volume, with the same surface area and height and with the same volume and height as that of trapezoidal solar pond are 0.294 m^2, 0.415 m^2 and 0.306 m^2 respectively in the month of June, 2016. It was noticed that the square solar pond with the same surface area and volume has lowest value among the three square solar ponds because shading area has depends on the surface area and height of solar pond and in this square solar pond surface area are more and height of solar is nearly $1/2^{th}$ of the other two solar ponds. It was concluded from this figure that trapezoidal solar pond with double glass cover has minimum shading area among all the solar ponds and therefore trapezoidal solar pond is best opinion for performance of the solar pond because shading area always decreases the performance of the solar pond.

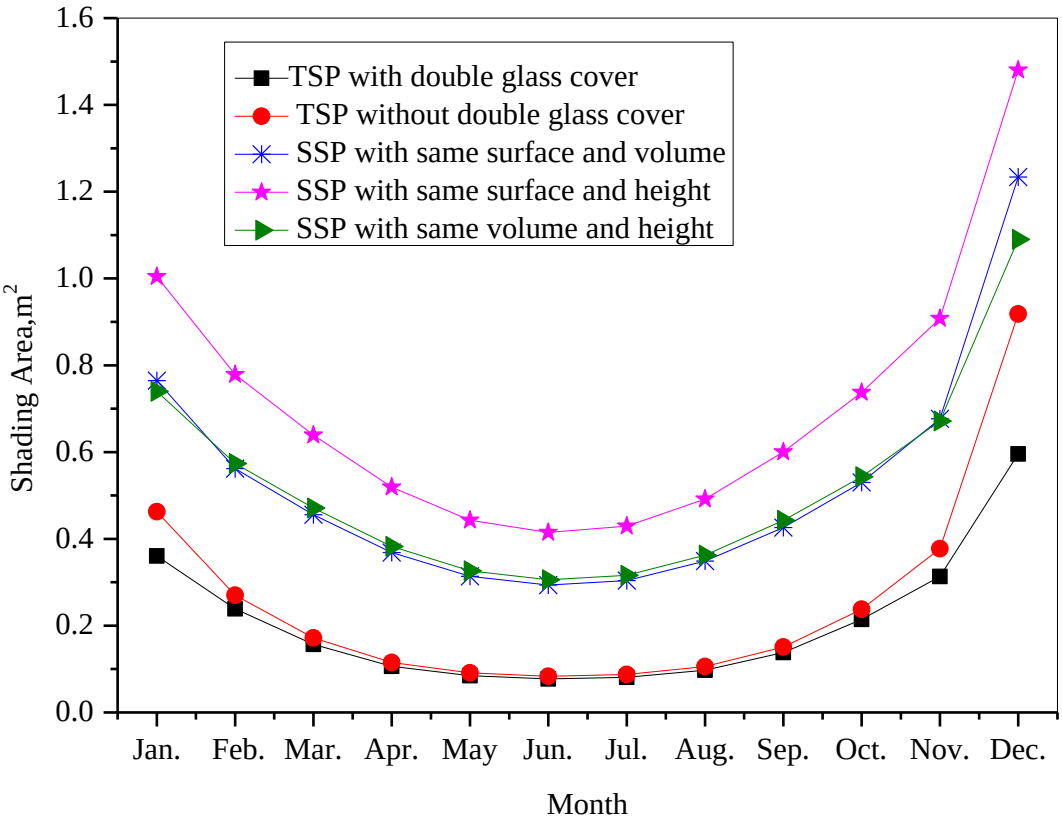

Fig 5.5 Comparison of the average shading area for various solar ponds

Figure 5.6 shows the layer-wise variation of shading area of trapezoidal solar pond at 12 pm, 3 pm and 5 pm on 15/04/2016. It can be seen that the shading area increases as the time progresses from 12 pm to 5 pm. The reason is that the incidence angle increases as time progresses in the afternoon. Similarly, shading area increases as the time decreases from 12 pm to 7 am because incidence angle increases from 12pm to 7am. The shading area of square solar pond increases almost linearly from top to bottom but in trapezoidal solar pond the rate of increase in shading area with depth decreases as shown in Figure 5.6. The reason is that the surface area of trapezoidal solar pond decreases with the depth of pond. As we know shading in the solar pond has continuously increases with the depth of solar pond but the shading area in the trapezoidal solar pond at 12 pm has decreases. The reason is that inclination angle of solar radiations is very small and refraction angle after solar radiation passes through water becomes more less as compared to incident angle and length of solar pond is continuously decreases towards the bottom side of solar pond. Therefore, the solar radiation reach to the side bottom of the trapezoidal solar pond but not reaches on upper side of trapezoidal solar pond. It is possible in the case of trapezoidal salt gradient solar pond but not in square solar pond.

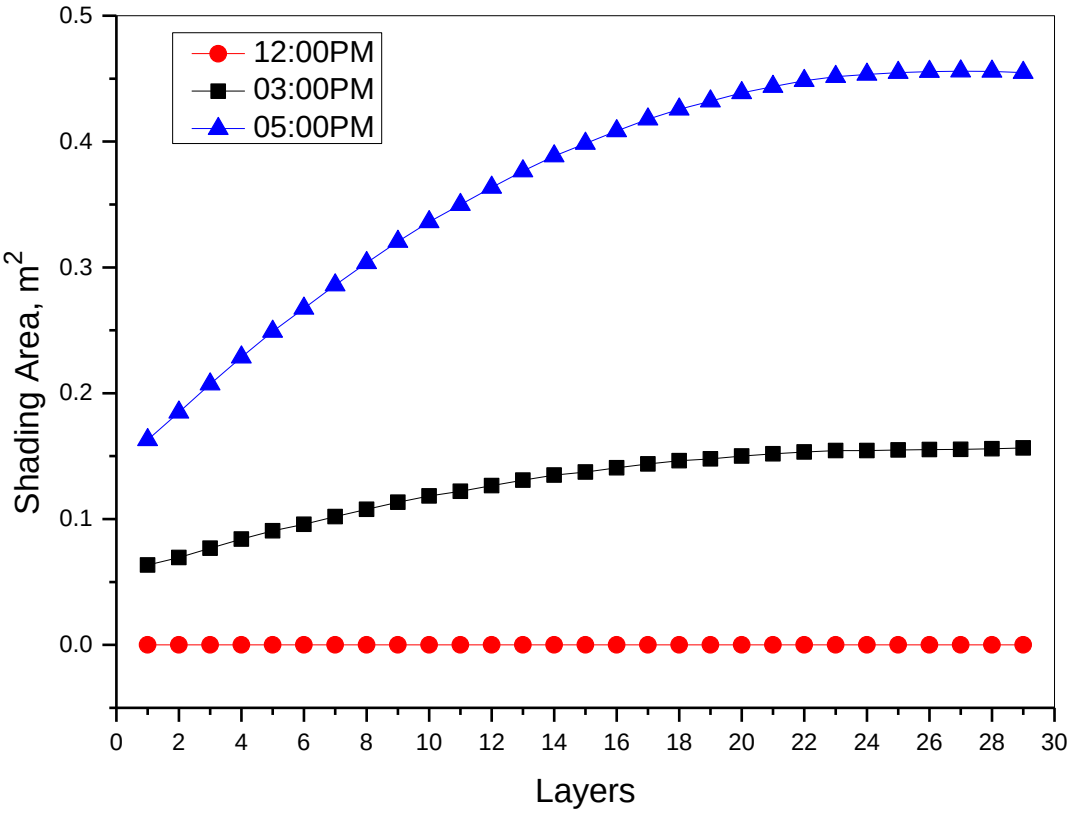

Fig 5.6 Shading area of different layers of trapezoidal solar pond on 15/04/2016

Figure 5.7 shows the hourly temperature distribution in LCZ of solar pond with and without double glass cover on 19/05/2016 and 20/04/2016. The temperature without double glass cover is little bit larger than with double glass solar pond because solar radiation is directly comes in bottom of the surface but in double glass cover the transmittance of glass for solar radiations is 0.89. Temperature is continuously increases throughout the day because of solar radiation falls on the surface of solar pond but at night temperature of the solar pond are decreases slowly.

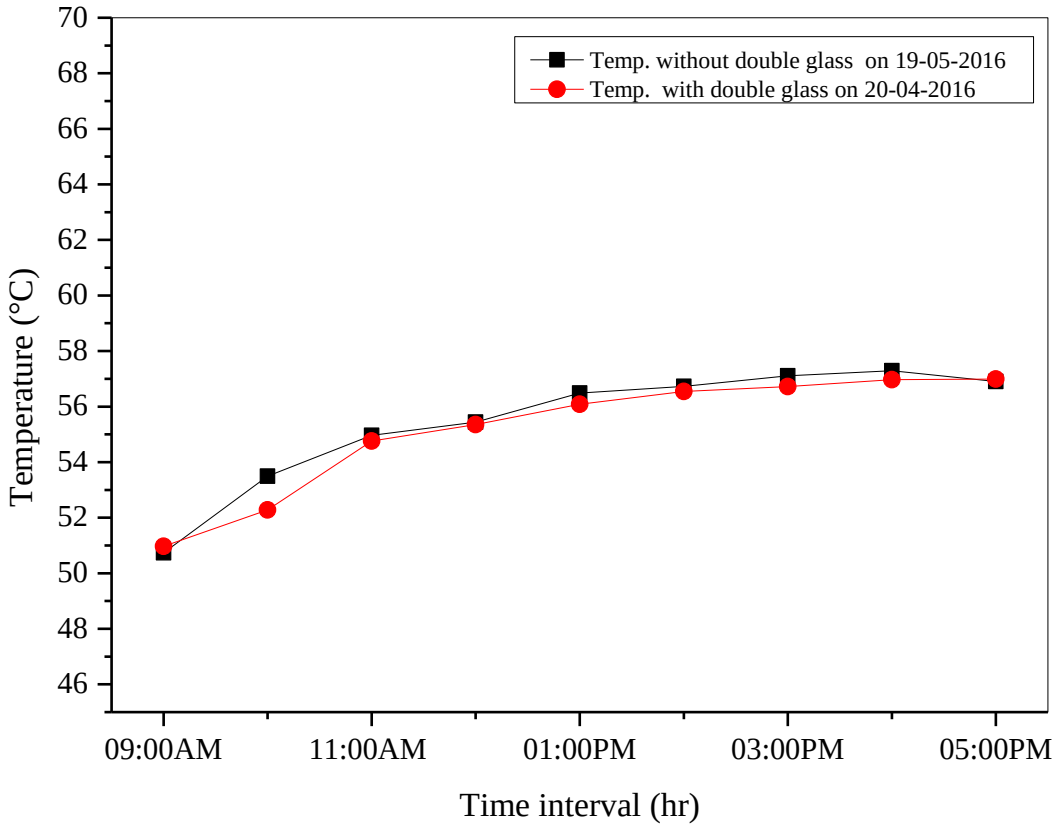

Figure 5.7 shows the hourly temperature distribution for LCZ with and without double glass cover on 19/05/2016 and 20/04/2016.

Figure 5.8 shows the hourly temperature distribution for NCZ with and without double glass cover on 19/05/2016 and 20/04/2016. The temperature with double glass cover solar pond is higher than the temperature without double glass cover solar pond throughout the day because the solar radiations have entrapped by the double glass but in solar without double glass cover convection and evaporation losses are continuously goes on throughout the day. Figure 5.9 shows the hourly temperature distribution for UCZ with and without double glass cover on 19/05/2016 and 20/04/2016. Maximum solar radiations are entrapped by double glass cover therefore temperature of solar with double glass is more than without double glass. Therefore, the solar pond with double glass cover has used for further application with full volume of water that contains the solar pond but in without double glass solar pond only $1/3^{th}$ volume of heated water is used for further applications because the volume of water in LCZ of solar pond without double glass has $1/3^{th}$ volume of total volume. Figure

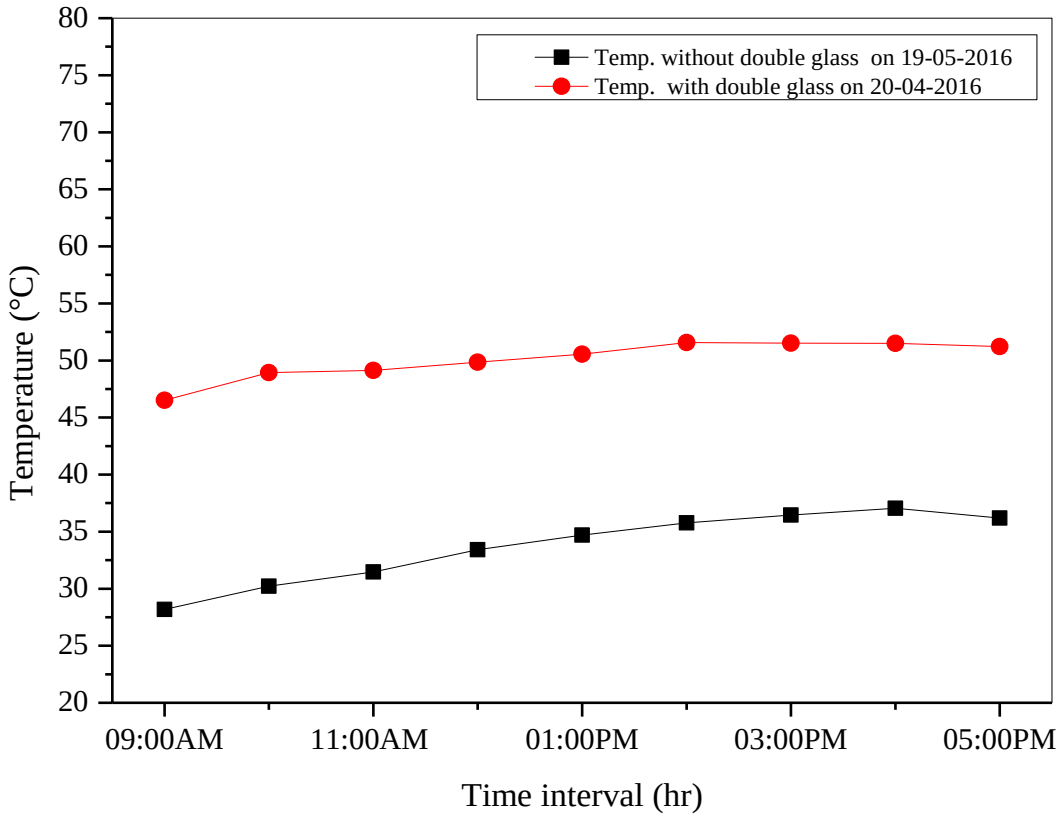

Figure 5.8 shows the hourly temperature distribution for NCZ with and without double glass cover on 19/05/2016 and 20/04/2016

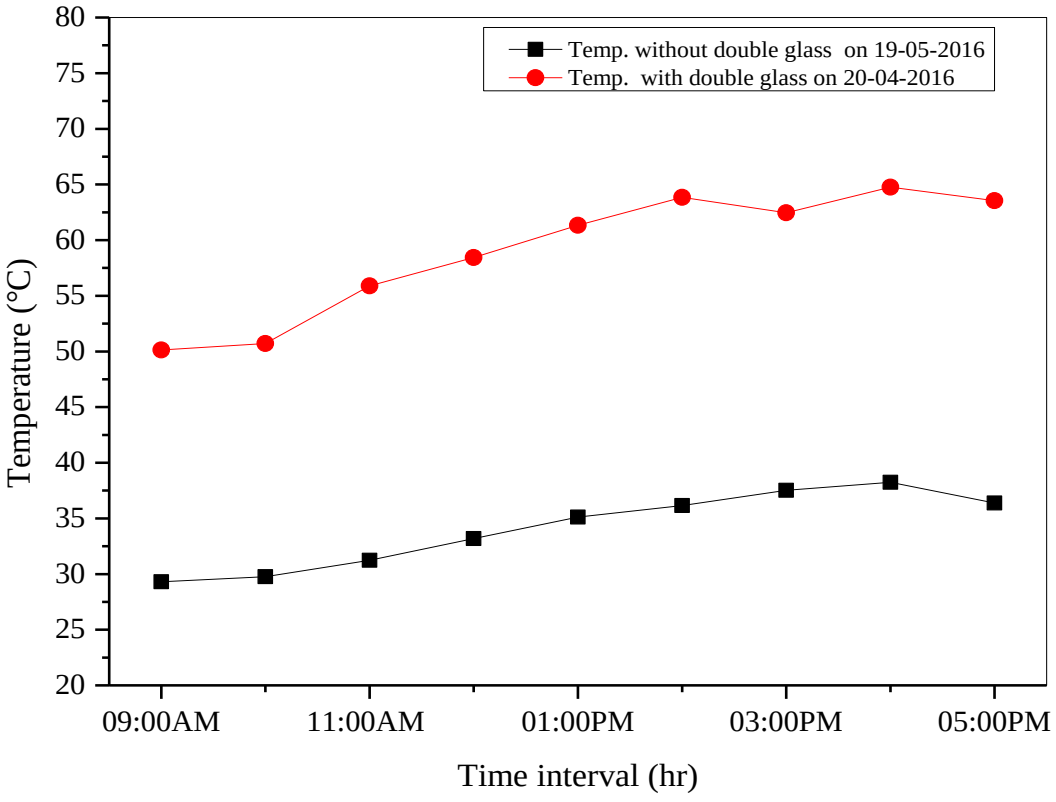

Figure 5.9 shows the hourly temperature distribution for UCZ with and without double glass cover on 19/05/2016 and 20/04/2016

Figure 5.10 shows the hourly variation of solar intensity on the top surface of the solar pond with and without using reflector on 01/05/2016. The reflector was placed south facing and inclined at an angle of 70° (optimum inclination angle on 01/05/2016) from the horizontal surface. The optimum inclination angle of 70° was calculated by using the procedure as explained in the section 3 (optimum inclination angle of reflector). It can be seen from the figure that the enhancement of solar intensity on the top surface of a solar pond due to reflector is significant during the time interval of 11 am to 2 pm and the enhancement of solar intensity is insignificant during the rest hours of the day. The reason is that the position of reflector is fixed to south facing and therefore only during 11 am to 2 pm, almost all the radiations reflected from the reflector fall on the pond surface and during the rest hours of the day, most of the radiations reflected from the reflector go away from the pond surface. The average solar intensity on the top surface of solar pond by using reflector with fixed position is increased by 22%.

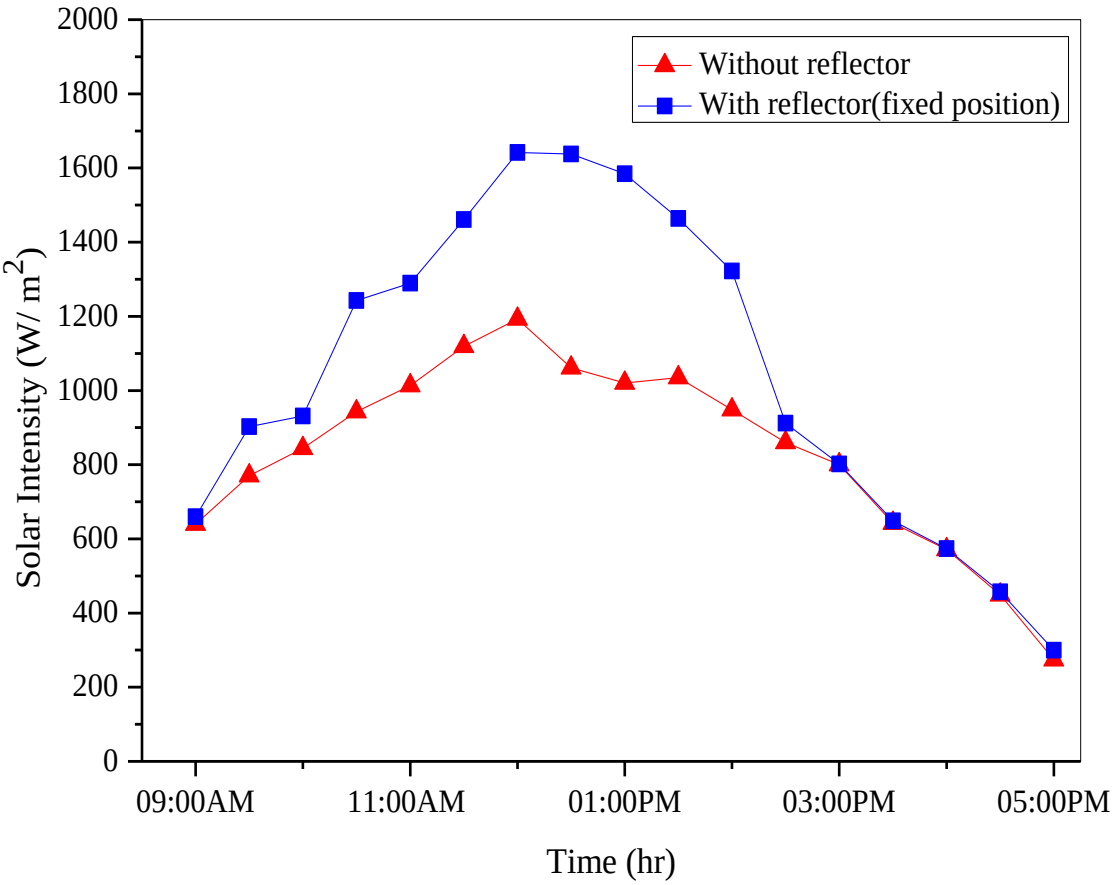

Figure 5.10 Comparison of the solar intensity on the top surface of solar pond with reflector (fixed position) and without reflector on 01/05/2016

Figure 5.11 shows the hourly variation of solar intensity on the top surface of the solar pond with reflector (fixed position) and without reflector on 14/05/2016. The reflector was inclined at an angle of 68° (optimum inclination angle on 14/05/2016) from the horizontal surface. In order to receive the maximum solar radiation on the reflector surface throughout the day, the reflector is positioned east facing during 9 am to 11 am, south facing during 11 am to 2 pm and west facing during 2 pm to 5 pm. Now, it can be noticed that the enhancement of solar intensity on top surface of solar pond is significant throughout the day. The average solar intensity on the top surface of solar pond by using reflector with changing position is increased by 47%.

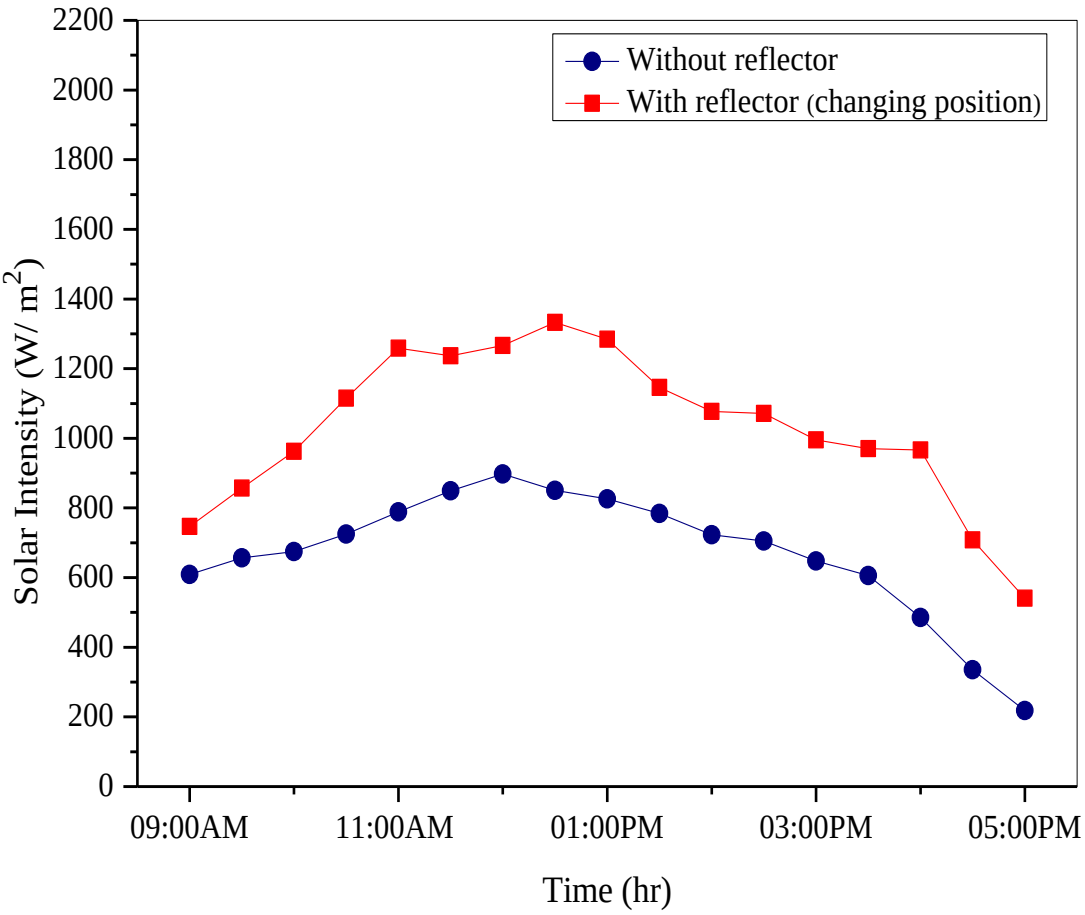

Figure 5.11 Comparison of the solar intensity on the top surface of solar pond with reflector (changing position) and without reflector on 14/05/2016

Figure 5.12 shows the temperature distribution in various trapezoidal solar ponds. It can be noticed that the solar pond without double glass cover attains temperature only in the lower convective zone because thermal losses continuously takes place from the top surface of solar

pond. Whereas, the solar ponds with double glass cover attain temperature in all the three zones because the thermal energy remain trapped inside the pond. Further, it can also be observed that the highest average temperature in the solar pond is achieved when the solar pond is covered with double glass cover and coupled with reflector (changing position). The average temperature in solar pond without double glass cover and without reflector, with double glass cover and without reflector, with double glass cover and with reflector (fixed position) and with double glass cover and with reflector (changing position) are 44.2 °C, 55.1 °C, 65.4 °C and 70.5 °C, respectively.

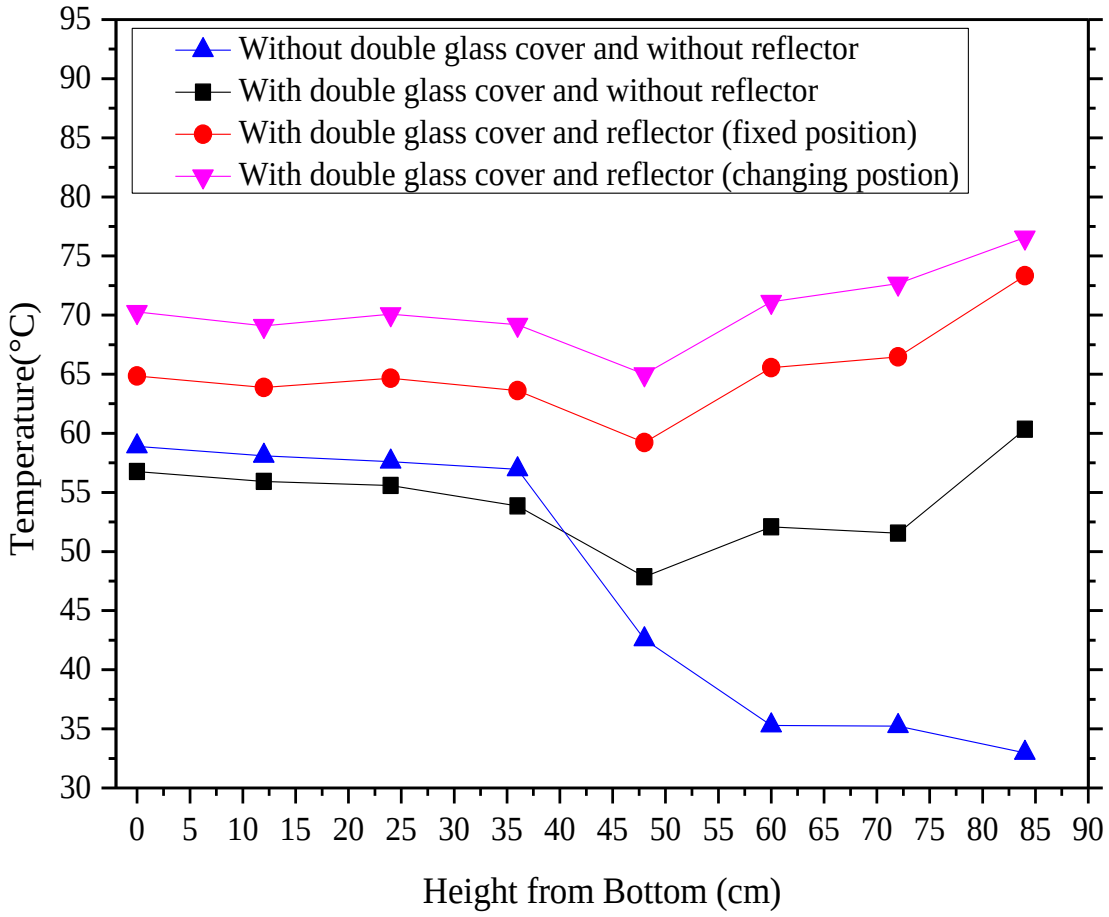

Figure 5.12 Temperature distribution in various trapezoidal solar ponds

Figure 5.13 shows the temperature distribution in the solar pond from 23/03/2016 to 27/05/2016. On 23/03/2015 solar pond was covered with double glass and temperature in the solar pond is continuously increases day by day. It was noticed that, in a day, average increase in the temperature of the solar pond by 1.58 °C. This solar pond attains the maximum optimum temperature throughout the volume with double glass cover was 55 °C. This temperature gains within 20 days then the temperature of solar doesn't increase because

temperature gain in the day time becomes equals to the thermal losses during the night. Therefore solar pond was coupled with the reflector to increase the performance of the solar pond. Reflector (Fixed position) increase the solar pond temperature by 10 °C and Reflector (Changing position) increase the solar pond temperature by 15 °C. Then remove double glass cover and reflector to determine the solar pond performance without reflector and double glass cover. Further, it was noticed that the increases in the LCZ because direct solar radiation at the bottom surface and upper layer temperature value was close to atmosphere temperature because continuously evaporation of water takes place which reduces the temperature of the solar pond. The average solar pond temperature without double glass and reflector was noticed near about 44 °C.

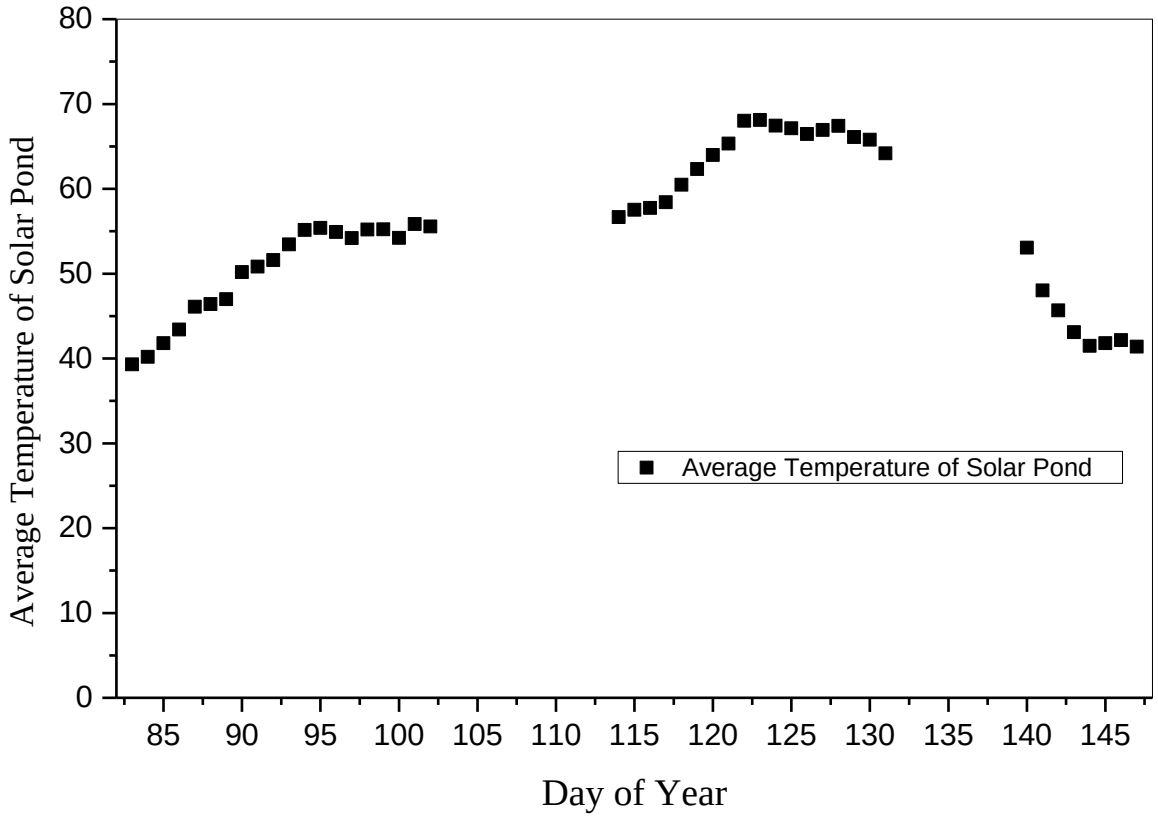

Figure 5.13 Average temperature distribution of solar pond with the day of the year

Figure 5.14 show the thermal efficiencies of LCZ, NCZ and UCZ for the three trapezoidal solar ponds i.e., trapezoidal solar pond without double glass cover and without reflector, with double glass cover and without reflector and with double glass cover and with reflector. The thermal efficiencies of LCZ, NCZ and UCZ for the TSGSP without double glass cover and without reflector are 24.34 %, 12.12% and 1.32%, respectively. The thermal efficiencies of LCZ, NCZ and UCZ for the TSGSP with double glass cover and without reflector are

29.68%, 21.56% and 5.17%, respectively. The thermal efficiencies of LCZ, NCZ and UCZ for the TSGSP with double glass cover and with reflector are 32.73%, 23.22% and 5.30%, respectively.

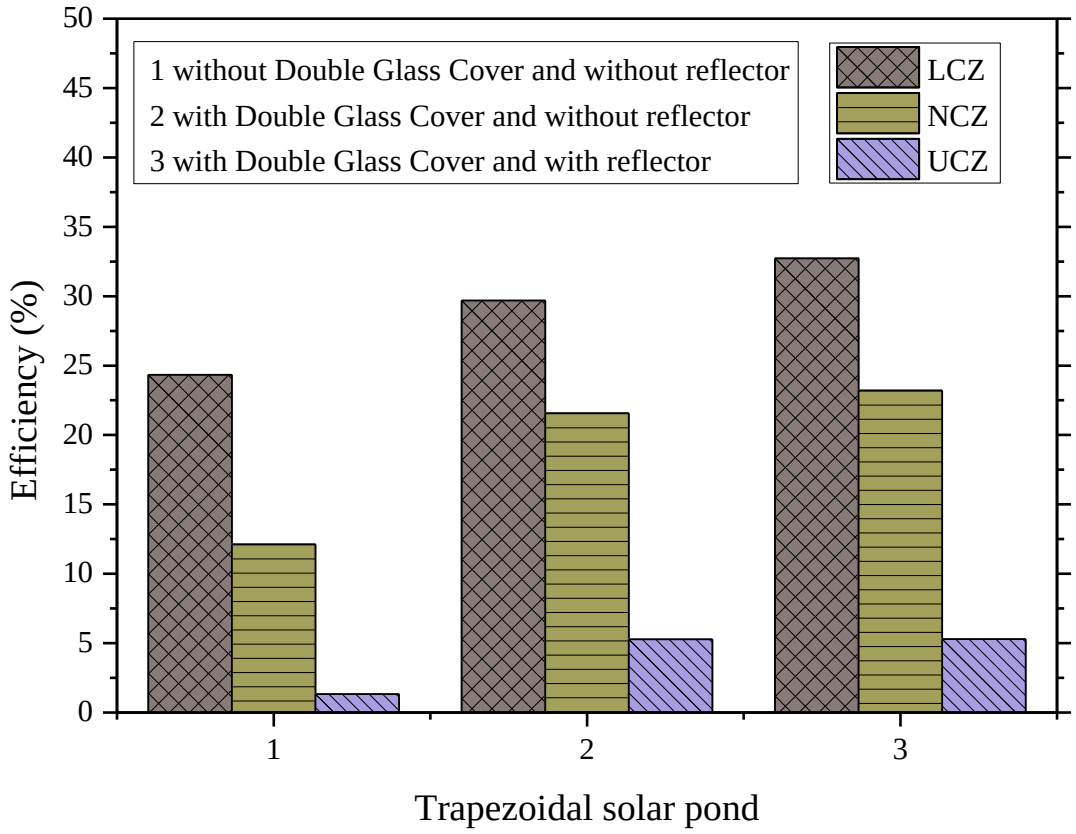

Figure 5.14 Thermal efficiencies of LCZ, NCZ and UCZ for the trapezoidal solar

Chapter 6

Conclusions and Future Scope

6.1 Conclusions

The following conclusions have been determined from the above mentioned study:

1. The solar ponds covered with glass cover are more energy efficient because the top losses are significantly reduced. Moreover, the solar pond with double glass cover attain temperature in all the three zones, therefore the solar pond with double glass cover can store more energy in comparison to the solar pond without double glass cover.
2. The response time of glass covered solar pond was relatively quick. It was observed that the maximum stable temperature in case of glass covered solar pond was attained in about 20 days, whereas the maximum stable temperature in case of solar pond without glass cover was attained in about 40 days.
3. Out of all the configurations and cases of solar ponds studied in this work, the trapezoidal solar pond with double glass cover has the highest sunny area ratio of 94.12%.
4. The use of reflector increases the rise of temperature in solar pond. The average temperature of trapezoidal solar pond with double glass cover is found to be 55 °C and this temperature is increased to 65.25 °C and 70.5 °C when solar pond with double glass cover is coupled with reflector (fixed position) and reflector (changing position), respectively.
5. The trapezoidal solar pond with double glass cover and reflector was found to be most thermally efficient among the three configurations of trapezoidal solar pond studied in the present work. The thermal efficiencies of LCZ, NCZ and UCZ for the trapezoidal solar pond with double glass cover and with reflector were 32.73%, 23.22% and 5.30%, respectively.

6.2 Future Scope

1 In the present study, a mathematical modelling is done to determine the shading area in the solar pond. The same mathematical modelling can be further extended to determine the effect of shading area on the thermal performance of the solar pond.

2 In the present study, the thermal losses through the side walls of the solar pond are not estimated. Since determination of thermal losses from the solar pond surfaces is essential to estimate the thermal performance of the solar pond, therefore the temperatures should be measured on the side walls in future work by fixing thermocouples in order to finally use these values to determine the thermal performance of the solar pond.

3 In the present study, the position and inclination of reflector is changed manually. The reflector system with an automatic control can be develop in the future which will adjust the inclination and change the position automatically.

4 The heat storage capability of solar pond is studied in the present work. This study can be further extended to utilise and transfer the stored heat to some thermal system by employing the heat exchanger.

References

[1] B. Schober and B. Schober, “DEPARTMENT OF TECHNOLOGY AND BUILT ENVIRONMENT,” no. June, 2010.

[2] B. Singh, J. Gomes, L. Tan, A. Date, and A. Akbarzadeh, “Small scale power generation using low grade heat from solar pond,” *Procedia Eng.*, vol. 49, pp. 50–56, 2012.

[3] A. Abdulsalam, A. Idris, T. A. Mohamed, and A. Ahsan, “The development and applications of solar pond: a review,” *Desalin. Water Treat.*, vol. 53, no. 9, pp. 2437–2449, 2015.

[4] H. Weinberger, “The physics of the solar pond,” *Sol. Energy*, vol. 8, no. 2, pp. 45–56, 1964.

[5] H. Kurt, M. Ozkaymak, and A. K. Binark, “Experimental and numerical analysis of sodium-carbonate salt gradient solar-pond performance under simulated solar-radiation,” *Appl. Energy*, vol. 83, no. 4, pp. 324–342, 2006.

[6] I. Bozkurt, S. Deniz, M. Karakilcik, and I. Dincer, “Performance assessment of a magnesium chloride saturated solar pond,” *Renew. Energy*, vol. 78, pp. 35–41, 2015.

[7] M. Mazidi, M. H. Shojaeefard, M. S. Mazidi, and H. Shojaeefard, “Two-dimensional modeling of a salt-gradient solar pond with wall shading effect and thermo-physical properties dependent on temperature and concentration,” *J. Therm. Sci.*, vol. 20, no. 4, pp. 362–370, 2011.

[8] M. A. Al-Dabbas, “Optimum Salt-Gradient Solar Pond in Jordan,” *Appl. Sol. Energy*, vol. 47, no. 1, pp. 14–23, 2011.

[9] M. Karakilcik, K. Kiyma??, and I. Dincer, “Experimental and theoretical temperature distributions in a solar pond,” *Int. J. Heat Mass Transf.*, vol. 49, no. 5–6, pp. 825–835, 2006.

[10] I. Bozkurt, S. Mantar, and M. Karakilcik, “A new performance model to determine energy storage efficiencies of a solar pond,” *Heat Mass Transf. und Stoffuebertragung*,

vol. 51, no. 1, pp. 39–48, 2014.

[11] M. Karakilcik, I. Dincer, I. Bozkurt, and A. Atiz, “Performance assessment of a solar pond with and without shading effect,” *Energy Convers. Manag.*, vol. 65, pp. 98–107, 2013.

[12] I. Bozkurt and M. Karakilcik, “The effect of sunny area ratios on the thermal performance of solar ponds,” *Energy Convers. Manag.*, vol. 91, pp. 323–332, 2015.

[13] M. Karakilcik, I. Dincer, and M. A. Rosen, “Performance investigation of a solar pond,” *Appl. Therm. Eng.*, vol. 26, no. 7, pp. 727–735, 2006.

[14] N. Ç. Bezir, O. Dönmez, R. Kayali, and N. Özek, “Numerical and experimental analysis of a salt gradient solar pond performance with or without reflective covered surface,” *Appl. Energy*, vol. 85, no. 11, pp. 1102–1112, 2008.

[15] N. Ç. Bezir, N. Özek, R. Kayalı, a. K. Yakut, a. Sencan, and S. Kalogirou, “Theoretical and Experimental Analysis of a Salt Gradient Solar Pond with Insulated and Reflective Covers,” *Energy Sources, Part A Recover. Util. Environ. Eff.*, vol. 31, no. 12, pp. 985–1003, 2009.

[16] I. Bozkurt, A. Atiz, M. Karakilcik, and I. Dincer, “An Investigation of the Effect of Transparent Covers on the Performance of Cylindrical Solar Ponds,” *Int. J. Green Energy*, vol. 11, no. 4, pp. 404–416, 2014.

[17] A. A. El-Sebaii, S. Aboul-Enein, M. R. I. Ramadan, and A. M. Khallaf, “Thermal performance of shallow solar pond under open cycle continuous flow heating mode for heat extraction,” *Energy Convers. Manag.*, vol. 47, no. 7–8, pp. 1014–1031, 2006.

[18] M. Husain, G. Sharma, and S. K. Samdarshi, “Innovative design of non-convective zone of salt gradient solar pond for optimum thermal performance and stability,” *Appl. Energy*, vol. 93, pp. 357–363, 2012.

[19] A. K. Saxena, S. Sugandhi, and M. Husain, “Significant depth of ground water table for thermal performance of salt gradient solar pond,” *Renew. Energy*, vol. 34, no. 3, pp. 790–793, 2009.

[20] A. A. Dehghan, A. Movahedi, and M. Mazidi, “Experimental investigation of energy

and exergy performance of square and circular solar ponds," *Sol. Energy*, vol. 97, pp. 273–284, 2013.

[21] A. Sakhrieh and A. Al-Salaymeh, "Experimental and numerical investigations of salt gradient solar pond under Jordanian climate conditions," *Energy Convers. Manag.*, vol. 65, pp. 725–728, 2013.

[22] R. S. Beniwal, R. V. Singh, and D. R. Chaudhary, "Heat losses from a salt-gradient solar pond," *Appl. Energy*, vol. 19, no. 4, pp. 273–285, 1985.

[23] A. A. El-Sebaii, M. R. I. Ramadan, S. Aboul-Enein, and A. M. Khallaf, "History of the solar ponds: A review study," *Renew. Sustain. Energy Rev.*, vol. 15, no. 6, pp. 3319–3325, 2011.

[24] M. R. I. Ramadan and A. M. Khallaf, "Experimental testing of a shallow solar pond with continuous heat extraction," vol. 36, pp. 955–964, 2004.

[25] A. Kumar and V. V. N. Kishore, "CONSTRUCTION AND OPERATIONAL EXPERIENCE OF A 6000 m2 SOLAR POND AT KUTCH, INDIA," *Sol. Energy*, vol. 65, no. 4, pp. 237–249, 1999.

[26] L. Hongsheng, J. Linsong, W. Dan, and S. Wence, "ScienceDirect Experiment and simulation study of a trapezoidal salt gradient solar pond," *Sol. ENERGY*, vol. 122, pp. 1225–1234, 2015.

[27] J. R. Hull, "Physics of the solar pond," 1979.

[28] M. R. Jaefarzadeh, "Thermal behavior of a small salinity-gradient solar pond with wall shading effect," *Sol. Energy*, vol. 77, no. 3, pp. 281–290, 2004.

[29] https://images-na.ssl-images-amazon.com/images/I/41in2alk5cL.jpg

Appendix A : MATLAB Scripts

MATLAB Script A1: The shading area of a trapezoidal salt gradient solar pond with double glass cover was evaluated as below:

```
“clc; % clc clears all the values in the Command Window display.
clear all;% clear all clears all objects in the workspace and close the engine.
close all; %close all deletes all figures whose handles are not hidden.
l = 30.3568;% Latitude of solar pond location
len=[1.533,1.505,1.476,1.448,1.419,1.391,1.362,1.334,1.306,1.277,1.249,1.220,1.192,1.163,1.135,1.106,1.078,1.049,1.021,0.993,0.964,0.936,0.907,0.879,0.850,0.822,0.795,0.767,0.738,0.711];%        different lengths of the solar which changes with the depth of the solar pond.
R=[0.047,0.062,0.076,0.090,0.104,0.119,0.133,0.147,0.161,0.175,0.190,0.204,0.218,0.232,0.247,0.261,0.275,0.289,0.304,0.318,
0.332,0.346,0.360,0.375,0.389,0.403,0.417,0.430,0.442,0.453];%  this is the horizontal distance between normal and the side surface of solar pond at i^th layer.
for M=1:1:12; % for the different months of the year
if M == 1
    n =1:1:31; % days in the month of January
elseif M == 2
    n =32:1:60;
elseif M == 3
    n =61:1:91;
elseif M == 4
    n =92:1:121;
elseif M == 5
    n =122:1:152;
elseif M == 6
    n =153:1:183;
elseif M == 7
```

```
    n =184:1:213;
elseif M == 8
    n =214:1:244;
elseif M == 9
    n =245:1:274;
elseif M == 10
    n =275:1:305;
elseif M == 11
    n =306:1:335;
elseif M == 12
     n =336:1:366;
end
t=9:1:17;   % local solar time from 9 am to 5 pm
x=1:1:30;   % 30 layers of solar pond with depth of solar pond
p=length(t); % no of values in the t
m=length(x); % no. of values in the x
q=length(n); % no. of values in the n
S=0;         % sum of shading initial is zero
MS=0;      % sum of shading area of months is zero at starting
for k=1:q
d = 23.45*sind((360/365.25)*(284+n(k))); % declination angle
for i=1:p
      h=(t(i)-12)*15; % hour angle
      Z=acosd((cosd(d)*cosd(l)*cosd(h))+(sind(d)*sind(l))); % Zenith
angle
      r=asind((1/1.33)*sind(Z));%Refraction angle from air to water
    r1=asind((2/3)*sind(Z));%Refraction angle from air to glas
for j=1:m
          sum(1)=0;
          S(j)=((((0.11+((x(j)-1)*0.03))*tand(r))-
R(j))*len(j))+(0.01*(tand(Z)+tand(r1))*1.58);
          if S(j) < 0
          S(j)=(0.01*(tand(Z)+tand(r1))*1.58);
```

```
            end;
            sum(j+1)=S(j)+sum(j);
            sum(j)=sum(j+1);
            X(i,j)=S(j);
            Y(i,j)= max(sum(j));
shading_depth=  (X(i,j));%  Shading  area  in  the  solar  pond  for
particular layer
end
DS(1)=0;
HAS(i)=Y(i,j)/m;%hourly average shading area in the solar pond
Dis(HAS(i));
DS(i+1)=DS(i)+HAS(i);  %  total  Shading  area  in  the  solar  pond  for
particular day
DS(i)=DS(i+1);
K(k,i)= max(DS(i));
end
HAS(i) =  Y(i,j)/m;
DS=K(k,i);
DAS(k)=K(k,i)/p;% day average shading area in the solar pond
Dis(DAS(k));
MS=MS+DAS(k); % total Shading area in the solar pond for particular
month
end
DAS(k)=K(k,i)/p;
MS;
MAS(M)=MS/q;% Monthly average shading area in the solar pond
end
MAS(M)=MS/q “
```

MATLAB Script A2: The shading area of a trapezoidal salt gradient solar pond without double glass cover was evaluated as below:

```
“clc; % clc clears all the values in the Command Window display.
clear all;% clear all clears all objects in the workspace and close the engine.
close all; %close all deletes all figures whose handles are not hidden.
l = 30.3568;% Latitude of solar pond location
len=[1.533,1.505,1.476,1.448,1.419,1.391,1.362,1.334,1.306,1.277,1.249,1.220,1.192,1.163,1.135,1.106,1.078,1.049,1.021,0.993,0.964,0.936,0.907,0.879,0.850,0.822,0.795,0.767,0.738,0.711];%        different lengths of the solar which changes with the depth of the solar pond.
R=[0.047,0.062,0.076,0.090,0.104,0.119,0.133,0.147,0.161,0.175,0.190,0.204,0.218,0.232,0.247,0.261,0.275,0.289,0.304,0.318,
0.332,0.346,0.360,0.375,0.389,0.403,0.417,0.430,0.442,0.453];%  this is the horizontal distance between normal and the side surface of solar pond at i^th layer.
for M=1:1:12;  % for the different months of the year
if M == 1
    n =1:1:31; % days in the month of January
elseif M == 2
    n =32:1:60;
elseif M == 3
    n =61:1:91;
elseif M == 4
    n =92:1:121;
elseif M == 5
    n =122:1:152;
elseif M == 6
    n =153:1:183;
elseif M == 7
    n =184:1:213;
elseif M == 8
```

```
    n =214:1:244;
elseif M == 9
    n =245:1:274;
elseif M == 10
    n =275:1:305;
elseif M == 11
    n =306:1:335;
elseif M == 12
     n =336:1:366;
end
t=9:1:17;   % local solar time from 9 am to 5 pm
x=1:1:30;   % 30 layers of solar pond with depth of solar pond
p=length(t);% no of values in the t
m=length(x);% no. of values in the x
q=length (n); % no. of values in the n
S=0;         % sum of shading initial is zero
MS=0;      % sum of shading area of months is zero at starting
for k=1:q
d = 23.45*sind((360/365.25)*(284+n(k))); % declination angle
for i=1:p
      h=(t(i)-12)*15; % hour angle
      Z=acosd((cosd(d)*cosd(l)*cosd(h))+(sind(d)*sind(l))); % Zenith
angle
      r=asind((1/1.33)*sind(Z));% Refraction angle from air to water
   r1=asind((2/3)*sind(Z));%Refraction angle from air to glass
for j=1:m
          sum(1)=0;
           S(j)=((((0.11+((x(j)-1)*0.03))*tand(r))-
           R(j))*len(j))+ ((0.02*tand(Z))*1.58);
          if S(j) < 0
          S(j)=(0.01*(tand(Z)+tand(r1))*1.58);
          end;
          sum(j+1)=S(j)+sum(j);
```

```
            sum(j)=sum(j+1);
            X(i,j)=S(j);
            Y(i,j)= max(sum(j));
shading_depth=  (X(i,j));%  Shading  area  in  the  solar  pond  for
particular layer
end
DS(1)=0;
HAS(i)=Y(i,j)/m;%hourly average shading area in the solar pond
Dis(HAS(i));
DS(i+1)=DS(i)+HAS(i); % total Shading area in the solar pond for
particular day
DS(i)=DS(i+1);
K(k,i)= max(DS(i));
end
HAS(i) =  Y(i,j)/m;
DS=K(k,i);
DAS(k)=K(k,i)/p;% day average shading area in the solar pond
Dis(DAS(k));
MS=MS+DAS(k); % total Shading area in the solar pond for particular
month
end
DAS(k)=K(k,i)/p;
MS;
MAS(M)=MS/q;% Monthly average shading area in the solar pond
end
MAS(M)=MS/q “
```

MATLAB Script A3: The shading area of a square solar pond without double glass cover having the same surface and same volume as that of trapezoidal solar pond was evaluated as below:

```
“clc; % clc clears all the values in the Command Window display.
clear all;% clear all clears all objects in the workspace and close the engine.
close all; %close all deletes all figures whose handles are not hidden.
l = 30.3568;% Latitude of solar pond location
le=1.625; % Upper length of solar pond from where solar radiations enters in the solar pond
for M=1:1:12;  % for the different months of the year
if M == 1
    n =1:1:31; % days in the month of January
elseif M == 2
    n =32:1:60;
elseif M == 3
    n =61:1:91;
elseif M == 4
    n =92:1:121;
elseif M == 5
    n =122:1:152;
elseif M == 6
    n =153:1:183;
elseif M == 7
    n =184:1:213;
elseif M == 8
    n =214:1:244;
elseif M == 9
    n =245:1:274;
elseif M == 10
    n =275:1:305;
elseif M == 11
```

```
    n =306:1:335;
elseif M == 12
     n =336:1:366;
end
t=9:1:17;    % local solar time from 9 am to 5 pm
x=1:1:27;    % 27 layers of solar pond with depth of solar pond
p=length(t); % no of values in the t
m=length(x); % no. of values in the x
q=length(n); % no. of values in the n
S=0;         % sum of shading initial is zero
MS=0;      % sum of shading area of months is zero at starting
for k=1:q
d = 23.45*sind((360/365.25)*(284+n(k))); % declination angle
for i=1:p
      h=(t(i)-12)*15; % hour angle
      Z=acosd((cosd(d)*cosd(l)*cosd(h))+(sind(d)*sind(l))); % Zenith
angle
      r=asind((1/1.33)*sind(Z));% Refraction angle from air to water
      r1=asind((2/3)*sind(Z));  % Refraction angle from air to glass
for j=1:m
          sum(1)=0;

S(j)=((0.11+((x(j)1)*0.02))*tand(r))*le+((0.02*tand(Z))*le) ;
          sum(j+1)=S(j)+sum(j);
          sum(j)=sum(j+1);
          X(i,j)=S(j);
Y(i,j)= max(sum(j));
shading_depth=  (X(i,j));%  Shading  area  in  the  solar  pond  for
particular layer
end
DS(1)=0;
HAS(i) =  Y(i,j)/m;% hourly average shading area in the solar pond
Disp(HAS(i));
```

```
DS(i+1)=DS(i)+HAS(i); % total Shading area in the solar pond for particular day
DS(i)=DS(i+1);
K(k,i)= max(DS(i));
end
HAS(i) =  Y(i,j)/m;
DS=K(k,i);
DAS(k)=K(k,i)/p;% day average shading area in the solar pond
Dis(DAS(k));
MS=MS+DAS(k); % total Shading area in the solar pond for particular month
end
DAS(k)=K(k,i)/p;
MS;
MAS(M)=MS/q;% Monthly average shading area in the solar pond
end
MAS(M)=MS/q “
```

MATLAB Script A4: The shading area of a square solar pond without double glass cover having the same height and same volume was evaluated as below:

```
“clc; % clc clears all the values in the Command Window display.
clear all;% clear all clears all objects in the workspace and close the engine.
close all; %close all deletes all figures whose handles are not hidden.
l = 30.3568;% Latitude of solar pond location
le=1.197; % Upper length of solar pond from where solar radiations enters in the solar pond
for M=1:1:12;  % for the different months of the year
if M == 1
    n =1:1:31; % days in the month of January
elseif M == 2
    n =32:1:60;
elseif M == 3
    n =61:1:91;
elseif M == 4
    n =92:1:121;
elseif M == 5
    n =122:1:152;
elseif M == 6
    n =153:1:183;
elseif M == 7
    n =184:1:213;
elseif M == 8
    n =214:1:244;
elseif M == 9
    n =245:1:274;
elseif M == 10
    n =275:1:305;
elseif M == 11
    n =306:1:335;
```

```
elseif M == 12
     n =336:1:366;
end
t=9:1:17;    % local solar time from 9 am to 5 pm
x=1:1:30;   % 30 layers of solar pond with depth of solar pond
p=length(t); % no of values in the t
m=length(x); % no. of values in the x
q=length(n); % no. of values in the n
S=0;         % sum of shading initial is zero
MS=0;      % sum of shading area of months is zero at starting
for k=1:q
d = 23.45*sind((360/365.25)*(284+n(k))); % declination angle
for i=1:p
      h=(t(i)-12)*15; % hour angle
      Z=acosd((cosd(d)*cosd(l)*cosd(h))+(sind(d)*sind(l))); % Zenith
angle
      r=asind((1/1.33)*sind(Z));% Refraction angle from air to water
      r1=asind((2/3)*sind(Z)); % Refraction angle from air to glass
for j=1:m
          sum(1)=0;

S(j)=((0.11+((x(j)1)*0.03))*tand(r))*le+((0.02*tand(Z))*le) ;
          sum(j+1)=S(j)+sum(j);
          sum(j)=sum(j+1);
          X(i,j)=S(j);
Y(i,j)= max(sum(j));
shading_depth=  (X(i,j));%  Shading  area  in  the  solar  pond  for
particular layer
end
DS(1)=0;
HAS(i) =  Y(i,j)/m;% hourly average shading area in the solar pond
Dis(HAS(i));
```

```
DS(i+1)=DS(i)+HAS(i); % total Shading area in the solar pond for
particular day
DS(i)=DS(i+1);
K(k,i)= max(DS(i));
end
HAS(i) =  Y(i,j)/m;
DS=K(k,i);
DAS(k)=K(k,i)/p;% day average shading area in the solar pond
Dis(DAS(k));
MS=MS+DAS(k); % total Shading area in the solar pond for particular
month
end
DAS(k)=K(k,i)/p;
MS;
MAS(M)=MS/q;% Monthly average shading area in the solar pond
end
MAS(M)=MS/q “
```

MATLAB Script A5: The shading area of a square solar pond without double glass cover having the same height and same surface was evaluated as below:

```
“clc; % clc clears all the values in the Command Window display.
clear all;% clear all clears all objects in the workspace and close the engine.
close all; %close all deletes all figures whose handles are not hidden.
l = 30.3568;% Latitude of solar pond location
le=1.625; % Upper length of solar pond from where solar radiations enters in the solar pond
R=[0.047,0.062,0.076,0.090,0.104,0.119,0.133,0.147,0.161,0.175,0.190,0.204,0.218,0.232,0.247,0.261,0.275,0.289,0.304,0.318,
0.332,0.346,0.360,0.375,0.389,0.403,0.417,0.430,0.442,0.453];%  this is the horizontal distance between normal and the side surface of solar pond at ith layer.
for M=1:1:12;  % for the different months of the year
if M == 1
    n =1:1:31; % days in the month of January
elseif M == 2
    n =32:1:60;
elseif M == 3
    n =61:1:91;
elseif M == 4
    n =92:1:121;
elseif M == 5
    n =122:1:152;
elseif M == 6
    n =153:1:183;
elseif M == 7
    n =184:1:213;
elseif M == 8
    n =214:1:244;
```

```
elseif M == 9
    n =245:1:274;
elseif M == 10
    n =275:1:305;
elseif M == 11
    n =306:1:335;
elseif M == 12
     n =336:1:366;
end
t=9:1:17;    % local solar time from 9 am to 5 pm
x=1:1:30;   % 30 layers of solar pond with depth of solar pond
p=length(t); % no of values in the t
m=length(x); % no. of values in the x
q=length(n); % no. of values in the n
S=0;         % sum of shading initial is zero
MS=0;  % sum of shading area of months is zero at starting
for k=1:q
d = 23.45*sind((360/365.25)*(284+n(k))); % declination angle
for i=1:p
      h=(t(i)-12)*15; % hour angle
      Z=acosd((cosd(d)*cosd(l)*cosd(h))+(sind(d)*sind(l))); % Zenith
angle
      r=asind((1/1.33)*sind(Z));% Refraction angle from air to water
      r1=asind((2/3)*sind(Z)); % Refraction angle from air to glass
for j=1:m
          sum(1)=0;
         S(j)=((0.11+((x(j)-
1)*0.03))*tand(r))*le+((0.02*tand(Z))*le) ;
          sum(j+1)=S(j)+sum(j);
          sum(j)=sum(j+1);
          X(i,j)=S(j);
Y(i,j)= max(sum(j));
```

```
shading_depth=  (X(i,j));% Shading area in the solar pond for particular layer
end
DS(1)=0;
HAS(i) =  Y(i,j)/m;% hourly average shading area in the solar pond
Dis(HAS(i));
DS(i+1)=DS(i)+HAS(i); % total Shading area in the solar pond for particular day
DS(i)=DS(i+1);
K(k,i)= max(DS(i));
end
HAS(i) =  Y(i,j)/m;
DS=K(k,i);
DAS(k)=K(k,i)/p;% day average shading area in the solar pond
Dis(DAS(k));
MS=MS+DAS(k); % total Shading area in the solar pond for particular month
end
DAS(k)=K(k,i)/p;
MS;
MAS(M)=MS/q;% Monthly average shading area in the solar pond
end
MAS(M)=MS/q “
```

Appendix B: Table

Table B1: Shows the solar intensity/insolation (W/m^2) without reflector and with reflector (Fixed position)

Date	01/05/2016		02/05/2016		13/05/2016	
Time	Insolation without reflector	Insolation with reflector (Fixed position)	Insolation without reflector	Insolation with reflector (Fixed position)	Insolation without reflector	Insolation with reflector (Fixed position)
09:00 AM	621.75	671.4	602.25	665.2	480	495
09:30 AM	648	704.2	619.5	735.8	578	677
10:00 AM	697.5	746.3	699.75	830.8	633	698
10:30 AM	738.75	885.0	753.75	983.3	707	932
11:00 AM	772.5	1003.2	888.75	1144.6	760	967
11:30 AM	911.25	1066.0	971.25	1311.6	839	1096
12:00 PM	971.25	1157.8	943.5	1212.3	895	1231
12:30 PM	750	1003.8	986.25	1233.8	796	1228
13:00 PM	975.75	1232.9	928.5	1291.1	765	1188
13:30 PM	916.5	1060.3	788.25	1073.0	776	1098
14:00 PM	746.25	881.6	762.75	1057.2	711	992
14:30 PM	634.5	686.4	782.25	810.3	645	684
15:00 PM	663.75	664.4	585	634.7	601	601
15:30 PM	521.25	543.9	509.25	544.9	485	487
16:00 PM	415.5	416.2	396.75	425.1	428	430
16:30 PM	312.75	313.3	306	315.3	337	343
17:00 PM	222	223.2	190.5	198.5	206	225

Table B2: Shows the solar intensity/insolation (W/m^2) without reflector and with reflector (changing position)

Date	01/05/2016		02/05/2016	
Time	Insolation without reflector	Insolation with reflector (changing position)	Insolation without reflector	Insolation with reflector (changing position)
09:00 AM	609	747	609	1034
09:30 AM	657	857	657	1164
10:00 AM	675	962	675	1210
10:30 AM	725	1115	725	1242
11:00 AM	789	1259	803	1250
11:30 AM	803	1174	849	1249
12:00 PM	849	1237	898	1271
12:30 PM	898	1267	851	1182
13:00 PM	851	1333	826	1205
13:30 PM	826	1284	785	1178
14:00 PM	785	1146	723	1217
14:30 PM	724	837	705	1220
15:00 PM	723	1077	648	1209
15:30 PM	705	1072	606	1054
16:00 PM	648	995	485	1065
16:30 PM	606	970	335	832
17:00 PM	485	966	218	542

Table B3: Shows the yearly sunny area ratio (%) for different cases of solar ponds.

Month	Sunny area ratio (%)				
	TSP with double glass	TSP without double glass	SSP with same surface area & volume	Square SP with same surface area & height	Square SP with same surface area & height
January	72.606	64.842	71.045	61.967	48.367
February	81.851	79.473	78.721	70.515	59.974
March	88.073	86.949	82.743	75.794	67.134
April	91.917	91.233	86.045	80.330	73.297
May	93.573	93.064	88.120	83.224	77.227
June	94.120	93.657	88.878	84.288	78.671
July	93.831	93.345	88.488	83.739	77.924
August	92.593	91.978	86.795	81.376	74.721
September	89.509	88.559	83.871	77.259	69.124
October	83.712	81.912	79.933	72.063	62.074
November	76.214	71.322	74.385	65.610	53.148
December	54.769	30.246	53.280	43.953	23.912

Table B4: Shows the temperature distribution of solar pond with and without reflector and with and without double glass cover with height of solar from bottom.

Height from bottom (cm)	Without double glass cover and without reflector on 19/5/2016	With double glass cover and without reflector on 20/4/2016	With double glass cover and reflector (fixed position) on 30/4/2016	With double glass cover and reflector (changing position) 1/5/2016
0	58.9	56.77	64.85	70.28
12	58.1	55.93	63.87	69.1
24	57.6	55.58	64.66	70.08
36	56.96	53.86	63.62	69.18
48	42.58	47.86	59.21	65
60	35.29	52.09	65.55	71.13
72	35.23	51.56	66.46	72.66
84	32.97	60.34	73.34	76.57